POLITECNICO DI TORINO

Master's Degree in Mechatronics Engineering

Master's Degree Thesis

Development of a Low-Voltage Hybrid Storage System with GaN FET Converter

Supervisors:
Prof. Salvatore Musumeci
Dr. Luigi Solimene

Candidate:
Mohamad Khalife

October 2024

Abstract

This thesis presents the development of a low voltage storage system utilizing a Gallium Nitride (GaN) Field-Effect Transistor (FET) converter. The primary objective is to design a hybrid energy storage system (HESS) that integrates a supercapacitor and a lithium-ion battery to efficiently manage power distribution between these components. The system aims to leverage the high power density of supercapacitors and the high energy density of lithium-ion batteries to optimize performance during both charging and discharging cycles. The project employs PLECS software to model and simulate the behavior of the HESS. The PLECS environment allows for detailed analysis and optimization of the power management system, ensuring efficient energy transfer and storage. Additionally, MATLAB Simulink is used to support the integration of the HESS model, providing a robust platform for simulation and verification of the control strategies developed. Throughout this research, key focus areas include the design and implementation of control algorithms for power management, thermal management of the GaN FET converter, and the overall efficiency and reliability of the hybrid storage system. The findings demonstrate significant improvements in power efficiency and system stability, highlighting the potential of GaN FET technology in low voltage storage applications. The outcomes of this thesis contribute to the advancement of energy storage solutions, offering valuable insights into the practical application of hybrid storage systems and GaN FET converters in modern power management scenarios.

Acknowledgements

I would like to express my deepest gratitude to my family for their unwavering support throughout this journey. To my parents, Osman and Mona, your endless encouragement, patience, and understanding have been the cornerstone of my academic pursuits. Your sacrifices and belief in me have given me the strength to persevere, and for that, I am eternally grateful. I owe a special debt of gratitude to my professor Salvatore Musumeci and my supervisor Luigi Solimene your invaluable guidance, expertise, and patience have been instrumental in shaping the direction and quality of this research. Your insightful feedback and unwavering support have been crucial in overcoming the challenges I encountered along the way. I would also like to thank my colleagues and fellow students. Your camaraderie, collaboration, and constructive discussions have enriched my research experience. The shared moments of brainstorming and problem-solving have not only contributed to the success of this thesis but have also made this journey a memorable and enjoyable one. Thank you all for your contributions, encouragement, and unwavering support. This thesis would not have been possible without each and every one of you.

I would also like to extend my warmest thanks to all those who contributed to the success of this Thesis.

Contents

List of Figures

Chapter 1

Introduction

Ultracapacitors, also recognized as supercapacitors or electric double-layer capacitors, stand out as a promising energy storage technology with roots tracing back to the early 1950s. The pivotal work of scientists like H. Becker at General Electric during this period marked the inception of experiments with activated carbon as an electrode material. These early endeavors laid the groundwork for the development of double-layer capacitors, the fundamental mechanism underpinning ultracapacitors[6]. The commercialization of ultracapacitors gained significant traction in the 1970s and 1980s, with companies like NEC introducing them to the market. These energy storage devices operate on the principles of double-layer capacitance, occurring at the interface between an electrode and an electrolyte, and pseudo capacitance, arising from reversible redox reactions. The synergy of these mechanisms enables ultracapacitors to store and discharge electrical energy with exceptional power density, showcasing rapid charge and discharge capabilities, and exhibiting an extended cycle life[2]. Despite their remarkable attributes, ultracapacitors exhibit lower energy density compared to traditional batteries. However, their unique combination of features positions them as valuable components in applications that demand high power output, rapid energy transfer, and prolonged operational lifespans. As the field of energy storage continues to evolve, ultracapacitors emerge as a compelling solution, contributing to advancements in diverse industries and applications.

1.1 Construction and Operating Principle

The double sided coated electrodes are made from graphite carbon in the form of activated conductive carbon, carbon nanotubes or carbon gels. A porous paper

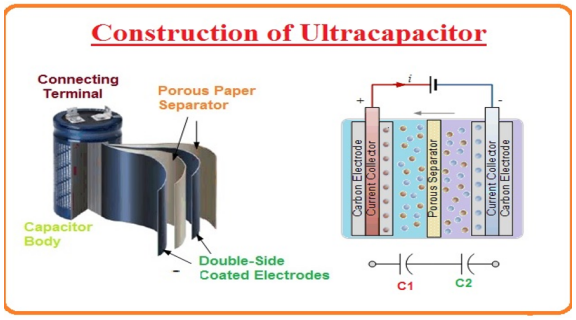

Figure 1.1: Construction of Ultracapacitor

membrane called a separator keeps the electrodes apart but allows positive ion to pass through while blocking the larger electrons. Both the paper separator and carbon electrodes are impregnated with the liquid electrolyte with an aluminum foil used in between the two to act as the current collector making electrical connection to the ultracapacitors solder tabs[3].

As we discussed in construction that this capacitor has two carbon films which are parted away with the insulating material. The dimension of this carbon sheet is such that it provides a larger area for charge storage. The extremely permeable carbon can stock a larger amount of energy than any other material capacitor. So, when the voltage provided at the +ve terminal it gets -ve ions toward them and voltage at the negative terminal attracts +ve ions toward them. This attraction makes a dual of coating of ions on both sides of the plate[21]. It is named as Double-layer creation. Due to this cause this capacitor also known as dual-layer capacitor. And the ions are then stowed near the outward of carbon. Ultra-capacitor stock energy by static charges on contrary outsides of the electrical dual film. They use the higher area of carbon for the energy storing substance, which causes higher energy storage than other normal capacitors. So The persistence of having partition is to stop the charges stirring around the electrodes. The quantity of energy stowed is very large as related to the typical capacitor.

- Molecular Viewpoint :

The structure of a supercapacitor resembles that of a battery, but it does not employ reactive materials. In batteries, there is an anode that charges negatively due to an oxidation reaction, where atoms lose electrons, leaving them free to conduct electricity and enter the electrolyte solution[8]. Conversely, the cathode undergoes reduction, where atoms gain electrons. This charge distribution creates a potential gradient, with an intermediate region of constant potential due to the electrolyte's inert nature[23]. The overall voltage across the battery is the open-

circuit voltage (V). Supercapacitors, on the other hand, use inert materials, so both positive and negative ions remain randomly distributed and do not undergo charge thickening. As a result, there is no voltage across the terminals. However, when a voltage is applied, electrons migrate from one electrode to the other, causing a physical shift in charge distribution. The electrode receiving electrons becomes positively charged, while the other electrode becomes negatively charged. This attracts ions of the opposite polarity, creating a double layer of charge akin to a conventional capacitor as shown in Figure 1.1. A negative ion in the electrolyte attracts solvent polar molecules, which exhibit both positive and negative charges but maintain overall neutrality due to their uneven distribution of charge. These polar molecules, acting as electric dipoles, interact with cations in the electrolyte, forming a surrounding cloud of charged particles near the electrode. This double layer of charge extends to a distance of just a few molecular layers, approximately 10 meters. This minute distance contributes significantly to the high capacitance of supercapacitors [9]. Moreover, the porous nature of carbon electrodes plays a crucial role in boosting capacitance. The vast surface area provided by these porous electrodes accommodates a large number of ions, further enhancing the capacity to store charge. The irregularities and crevices on the electrode surface increase the available space for ions to accumulate, further amplifying the capacitance. In summary, supercapacitors, unlike batteries, rely on charge shifting rather than chemical reactions to store energy. Their unique structure, featuring double-layer charging and porous carbon electrodes, enables them to achieve high energy density and fast charging/discharging capabilities, making them promising candidates for various applications.

i. Why Does Ultracapacitor have low energy density? :

Supercapacitors, excluding hybrid cells, employ a distinctive mechanism for energy storage by confining electrons onto insulating layers. The inherent challenge arises from the electrostatic repulsion among electrons, each bearing the same charge. This formidable repulsive force impedes efficient packing of electrons, and exceeding the optimal limit may lead to a disruptive phenomenon where electrons breach the insulating layer, escaping to the opposite terminal of the supercapacitor. This breakdown in the dielectric layer is catastrophic, creating an ionized path that facilitates the escape of numerous electrons, necessitating the maintenance of a relatively low energy density for supercapacitors [15].

In contrast, batteries store energy through the entrapment of electrons within

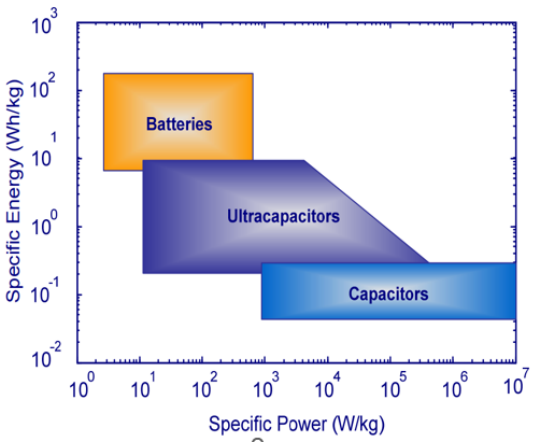

Figure 1.2: Ragione plot

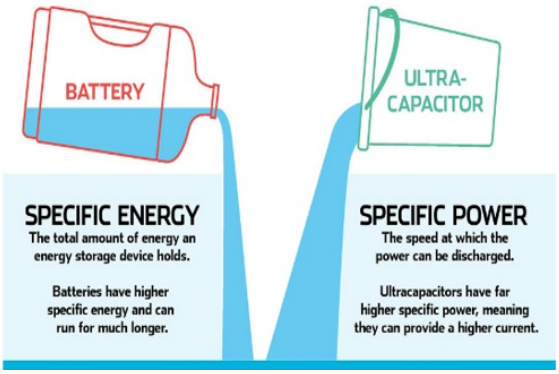

Figure 1.3: Main differences of Batteries and Supercapacitor

chemical bonds. The protons within these atoms are strategically configured, promoting a lower electron pressure and fostering content electrons that willingly coexist with protons. However, this chemical bonding introduces a caveat; the resulting compounds vary based on the number of electrons involved in their bonds, leading to chemical transformations influenced by factors such as heat, time, or the potential conversion into electron-impermeable compounds[11]. The selection of appropriate chemicals becomes a nuanced task due to the intricate interplay of these factors, underscoring the intricacies associated with energy storage in batteries.

1.2 Can Ultracapacitors Replace Batteries?

The answer to this question depends very much on what they will be used for. There are advantages and disadvantages to each. As previously mentioned, batteries have a much higher energy density than ultracapacitors. This means that they are more suitable for higher energy density applications, or when a device needs to run for long periods on a single charge. Ultracapacitors have a much higher power density than batteries. This makes them ideal for high-drain applications like powering an electric vehicle. As mentioned above, ultracapacitors also have a much longer lifespan than batteries. A regular battery can handle around 2000-3000 charge and discharge cycles, while ultracapacitors usually sustain over 1,000,000. This can represent considerable savings in materials and costs. Ultracapacitors are also much safer and considerably less toxic. They contain no harmful chemicals or heavy metals and are much less likely to explode than batteries[13]. In addition, ultracapacitors have a much greater operating range than batteries. In fact, they beat batteries hands down in this area, as they can operate within ranges of between -40 to +65 degrees Celsius. Many Ultracapacitor also have a much longer shelf life than batteries. Some, like SkelCap cells, can be stored for as long as 15 years at a time with little to no decline in capacity. As with most technology, the main driver for the application of ultracapacitors is their cost to benefit ratio. Ultracapacitors tend to be the more economical choice over the long run for applications needing short bursts of energy. Batteries, however, are a much better choice for applications that require constant, low current over time **Could ultracapacitors replace batteries in future electric cars? :**
As we have seen, ultracapacitors are best suited for situations where a lot of power is needed in a short period. In terms of electric cars, this would mean they would have advantages over batteries when the vehicle needs bursts of energy - like during acceleration. In fact, this is just what Toyota has done with the Yaris Hybrid-R concept car, which utilizes a supercapacitor for use during acceleration. [10] PSA Peugeot Citroen has also started employing ultracapacitors as part of its start-stop fuel-saving systems. This allows for much faster initial acceleration. Mazda's I-ELOOP system also uses ultracapacitors to store energy during deceleration. The power stored is then used for the engine's stop-start systems. Supercapacitors are also used to rapidly charge the power supplies in hybrid buses as they go from stop to stop.

When hybrid energy is used purely for performance, issues such as range and the ability to hold a charge aren't as important – and so some high-end manufacturers,

Figure 1.4: Tesla Supercharger Charging station for charging electric vehicles

such as Lamborghini are also starting to incorporate supercapacitor-powered e-motors in their hybrids. However, ultracapacitors are not a substitute for batteries in most electric vehicles - yet. Li-ion batteries will likely be the go-to power supply for EVs in the near to-distant future. Many believe it is more likely that ultracapacitors will become more commonplace as power-regeneration systems during deceleration. This stored power can then be re-used during periods of acceleration rather than direct replacements for batteries. However, according to this study, they could also have applications in hybrid vehicles in place of batteries when, "the power demand is less than the power capability of the electric motor; when the vehicle power demand exceeds that of the electric motor, the engine is operated to meet the vehicle power demand plus to provide the power to recharge the supercapacitor unit."

Recent research into graphene-based supercapacitors could also advance supercapacitor use in electric cars. One study by scientists at Rice University and the Queensland University of Technology resulted in two papers, published in the Journal of Power Sources and Nanotechnology. They proposed a solution consisting of two graphene layers, with an electrolyte layer between them. This resulting film is strong, thin, and able to release large amounts of energy in a short time. These factors are a given-it is a supercapacitor after all. This study is different because the researchers suggest that the new, thinner ultracapacitors could replace bulkier batteries in future electric vehicles. This could also include integrating the ultracapacitors into body panels, roof panelling, floors, and even doors. In theory, this could provide the vehicle with all the energy it needs and make it considerably lighter than battery-powered electric vehicles.

Chapter 2

Types of Ultracapacitor

There are a number of approaches being pursued to develop high energy density, high power capacitors suitable for use in vehicle applications. These approaches are identified in table 2.2 along with the basic chemistry/physics of the energy storage mechanisms, the materials used in the active electrodes, cell characteristics, and their potential performance (energy density, power density, etc.) [5]. Each of the capacitor types is described briefly in the following sections.

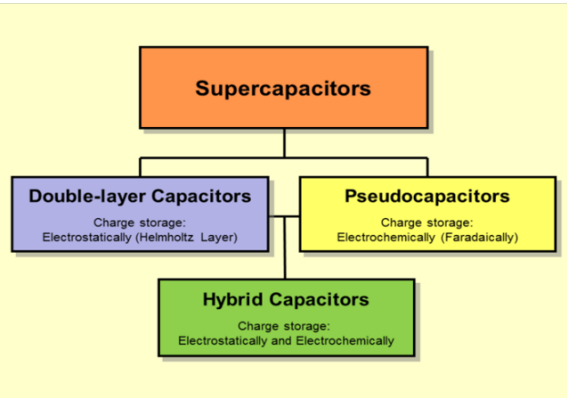

Figure 2.1: hierarchical classification of supercapacitors and capacitors of related types [24]

Technology type	Electrode materials	Energy storage mechanisms	Cell voltages	Energy density Wh/kg	Power density kW/kg
Electric double-layer	Activated carbon	Charge separation	2.5-3	5-7	1-3
Advanced carbon	Graphite carbon	Charge transfer or intercalation	3-3.5	8-12	1-2
Advanced carbon	Nanotube forest	Charge separation	2.5-3	not known	not known
Pseudo-capacitive	Metal oxides	Redox charge transfer	2-3.5	10-15	1-2
hybrid	Carbon/metal oxide	Double-layer/ charge transfer	2-3.3	10-15	1-2
Hybrid	Carbon/lead oxide	Double-layer/faradaic	1.5-2.2	10-12	1-2

Figure 2.2: Technology approaches for the development of high energy density electrochemical

2.1 Electrostatic double layered capacitors

The electrical double layer model of supercapacitors as shown in Figure 2.3 is first proposed by Helmholtz from German and developed as an electrical double layer theory by Gouy, Chapman and Stern, et al [14]. Helmholtz put forward the deduction of interface charge separation in the 19th century and designed the electrical double layer model like plate condenser based on the arrangement rules of positive and negative charges on two sides of rigid interface. This model is constituted of two opposite charge layers at an atomic distance and the potential varies linearly according to it. The capacitance Cd is supposed to remain constant whether the applied potential changes or not. However, since the model proposed by Helmholtz takes only the mutual effect of electrode and the absorbed layer into consideration without the effect of concentration of electrolyte, theoretical analysis matches the experiment results only when the electrolyte is concentrated and the potential difference is large enough, which calls for a modified model.

Characteristics of EDL:

- Electrical energy is stored by charge separation in the double layer.
- Electrodes are carbon electrodes or derivatives like charcoal powder rods.
- Charge is stored electrostatically.

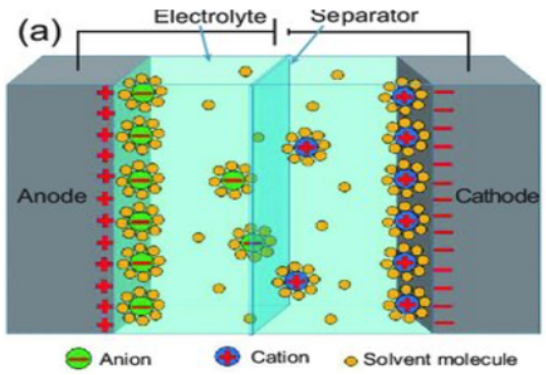

Figure 2.3: Representation of Electrical Double-Layer

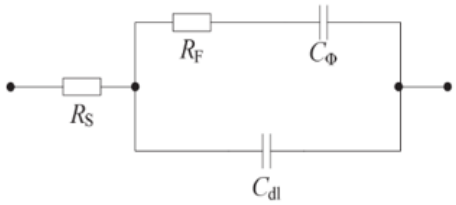

Figure 2.4: Coway Model

Figure 2.5: Maxwell 3000F SUPE

2.2 Pseudo-capacitor

Pseudo-capacitors (PC), unlike EDLC capacitors, make use of the redox reactions instead of the electrostatic attraction of the charges. These capacitors

undergo faradic reactions like the conventional batteries and the capacitance arises due to the electrochemical charge transfer. In PC too accompanied by the intercalation and deintercalation of charges just like batteries but the use of the electrolyte makes it more efficient in terms of power density. As the capacitance is based on the electrochemical nature it highly depends on the available active sites. In PC Figure the faradic charge storage is done at the electrodes. In this mechanism figure 2.6 there is a charge passage from the electrolyte to the electrode and vice versa in the charging and discharging process. This redox reaction between the electrolyte and the electrode is governed by thermodynamic properties and the potential window. In a PC the capacitance arises when a potential is applied, and it induces a faradaic current. This faradaic current is attributed to either electro-sorption or the redox reaction of the electrode materials. When the electro-sorption is in the play then it is governed by the chemisorption of anions while the redox reaction is governed by charge exchange from the double layer instead of the static charge separation. Thus, when the redox reaction takes place, both the EDLC and PC charge storing mechanism take place but with the selection of the proper material, the latter can be made to dominate over the former type of supercapacitor. These materials are usually the transition metal oxides and carbon-based material of nano porosity with electro-sorption hydrogen used. In PC the electro adsorbed charge is combined with the electrode potential controlling the extent of the charge sorption. This way the charge storage is dependent on the electrode potential and in turn the charge storing mechanism is controlled by the electron transfer instead of charge accumulation. But still, the pseudo capacitance cannot take place without the formation of the electric double layer which provides the ions from the charge transfer and is created due to the electrostatic attraction between the charged electrodes and the ions in the electrolyte.

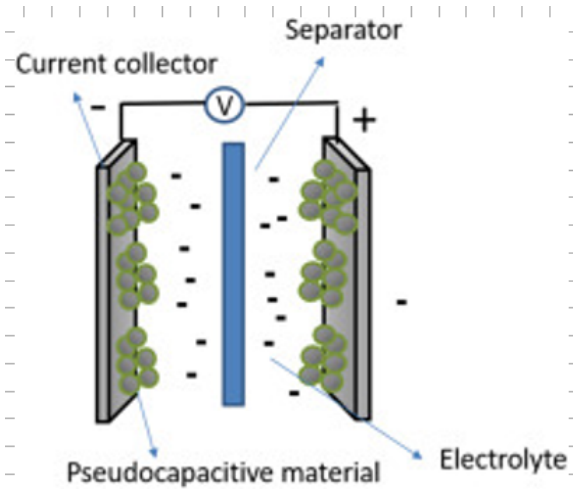

Figure 2.6: Schematic representation of pseudo-capacitors

The mechanism of charge and discharge of a pseudocapacitor is like the one of the batteries. During the charging process, the reaction at the cathode could be described as follows:

$$E_1 + A^- \xrightarrow{\text{charge}} E_1^{\delta+} \parallel A^- + \delta e^- \tag{2.1}$$

Moreover, the reaction at the anode is represented by:

$$E_2 + C^+ + \delta e^- \xrightarrow{\text{charge}} E_2^{\delta-} \parallel C^+ \tag{2.2}$$

E1 and E2 are the cathode and the anode, A and C+ represent the anion and cation, respectively, and // describes the electrolyte–electrode interface. The parameter e is the electrosorption valence, related to the oxidation-reduction reactions.

2.3 Hybrid Supercapacitors

This category of electrochemical capacitors refers to devices in which one of the electrodes is microporous carbon and the other electrode utilizes either a pseudocapacitance material or a Faradaic material like that used in a battery. These devices are often referred to as asymmetric capacitors. The charge/discharge characteristics of the hybrid capacitors have features of a double-layer capacitor (a linear voltage vs. time for a constant current charge/discharge) and that of a battery (voltage limits fixed by the potential of the battery-like electrode). the energy density of the hybrid capacitors utilizing intercalation carbon (graphite) in one of the electrodes is significantly higher than that of the carbon/carbon double-layer capacitors. However, even though the power density of those devices is relatively

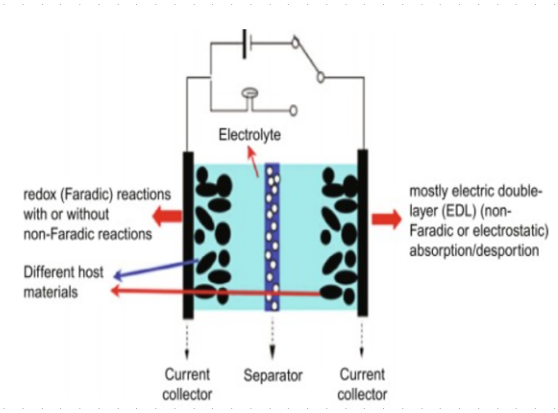

Figure 2.7: hybrid Supercapacitors

high (about 1000 W/kg, 95%), the power capability has not increased proportional to the increase in energy density.

This category(Hybrid supercapacitors) of electrochemical capacitors have recently come into focus and have progressed vastly [16]. They consist of two different types of electrode materials, a separator to isolate the two electrodes electrically, and an electrolyte. The structure of hybrid supercapacitors is illustrated schematically in Figure 2.7 To further enhance the energy density, hybrid supercapacitors usually comprise a redox (faradaic) reaction electrode or a battery-type electrode, with an electric double-layer electrode (typically carbon materials) in an organic or aqueous electrolyte . In such a hybrid supercapacitor, both mechanisms, electrical double-layer capacitance and faradaic or battery capacitance, happen simultaneously. The redox or battery-type electrodes have a large energy density, while the nonfaradaic capacitive electrode has high power density and excellent cycling stability . Thus, the electrode assembly can improve markedly the energy density of the device. In the field of hybrid capacitors, scientific and technical workers have developed both high voltage and high-energy density lithium and sodium ion capacitors [1].

Characteristics:

- Hybrid supercapacitors are combinations of both double layered and pseudo capacitor.
- The electrodes are asymmetric where one of the electrodes exhibits electrostatic property while the other exhibits electrochemical capacitance.
- Both pseudocapacitance and double layered capacitance make inseparable contributions to the full capacitance of hybrid supercapacitors.

2.4 Electrical and thermal characteristics of Ultracapacitor

1. ***Electrical Characteristics:***

   (a) **Capacitance (C)**: Ultracapacitors typically offer capacitance values ranging from a few farads to thousands of farads, allowing them to store and release large amounts of electrical charge.

   (b) **Voltage Rating (Vr)**: Ultracapacitors have voltage ratings ranging from a few volts to several hundred volts, indicating the maximum safe operating voltage.

   (c) **Energy Density (Wh/kg or Wh/L)**: Energy density is relatively lower than that of batteries but is typically measured in watt-hours per kilogram (Wh/kg) or watt-hours per liter (Wh/L).

   (d) **Power Density (W/kg or W/L)**: Ultracapacitors excel in power density, providing rapid charge and discharge capabilities, often measured in watts per kilogram (W/kg) or watts per liter (W/L).

   (e) **Equivalent Series Resistance (ESR)**: Ultracapacitors have low ESR values, which enable fast charge/discharge rates and minimize energy losses.

   (f) **Cycle Life**: Ultracapacitors offer a high cycle life, often exceeding hundreds of thousands to over a million charge/discharge cycles.

2. ***Thermal Characteristics:***

   (a) **Operating Temperature Range**: Ultracapacitors can operate efficiently within a wide temperature range, typically from -40°C to 65°C or higher, depending on the specific model and design.

   (b) **Self-Heating**: During rapid charge and discharge, ultracapacitors generate some self-heating due to their internal resistance (ESR). Proper thermal management is crucial for maintaining performance and safety in high-power applications.

   (c) **Thermal Runaway**: Like other electrical devices, ultracapacitors may experience thermal runaway if exposed to extreme conditions or abuse, making it essential to operate them within specified temperature and voltage limits.

(d) **Thermal Management**: Some high-power and high-energy applications may require thermal management systems, such as cooling or insulation, to maintain optimal operating conditions and prolong device lifespan.

2.5 Hybrid systems Battery-Supercapacitors introduction

The design and construction of electrochemical energy storage devices with higher energy and power density for multifunctional electronic devices, transport vehicles, and industrial equipment are of great importance. Within this agenda, the battery-supercapacitor hybrid (BSH) systems shown in Figure 2.8 comprising of high-rate capacitive and high-capacity battery electrodes have received extensive attention due to their exceptional performance as compared to conventional supercapacitors and batteries. With the appropriate and adept design, BSH (battery supercapacitor Hybrid) systems have inimitable benefits such as high productivity, low cost, security, and an eco-friendly process

Hybrid systems that combine batteries and supercapacitors (ultracapacitors) offer an innovative approach to energy storage and power management. These systems are designed to leverage the strengths of both technologies to optimize energy density, power density, and overall system performance as we mentioned above.So , The combination of lithium-ion battery (LiB) and ultracapacitor is often considered to be a superior choice for hybridization as it offers a trade-off between the desired criteria of high energy density and high power density with longer life time. In such hybridization, the UC can be responsible for delivering dynamic power demand while batteries supply constant energy. Moreover in HESS, the stress on the battery can be considerably minimized as the battery is not likely to respond during sharp load transients, thereby enhancing its cycle life.

A battery is often considered to be the good choice as energy storing element on account of its higher energy density and comparatively lower cost per watt hour [6]. However, the power demand for any vehicle is variable in nature as the transient power is demanded only during acceleration and braking for a very small duration of time as compared to the entire driving range. To store or release energy during these transients, an energy storing element with high dynamic charge acceptance capability is necessary. Besides, the charging/discharging lifetime, the cost and the weight are also the important parameters to be considered while choosing the energy source for EVs. Therefore, the performance characteristics required for most of the

EVs far exceed the capabilities of conventional battery based ESS.
Considering EV applications where the size and space of ESS is major concern, this research proposes a modified semi-active topology with a single bidirectional Dc-Dc converter for battery/ ultracapacitor hybridization.
The battery-UC HESS systems are broadly classified as:

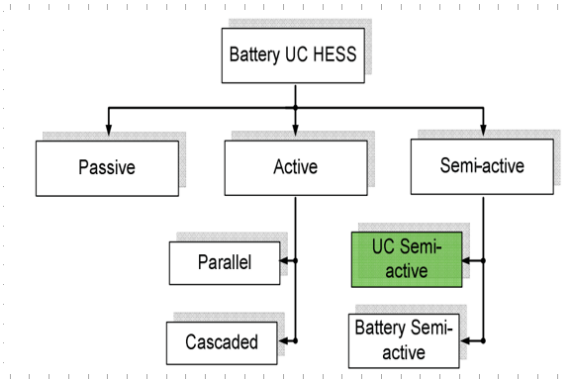

Figure 2.8: Conventional Topology used for hybridization

2.5.1 Passive HESS Configuration

The simplest configuration directly connects the energy sources in parallel. As illustrated in Figure 2.9, there is no DC/DC converter to decouple the battery and the ultracapacitor. Consequently, the HESS cannot be fully utilized to allocate the surge/slow currents between the storage systems. One of the key benefits that this configuration offers is reduced cost and minimal complexity due to the absence of any power electronic interface. Although the connection is quite simple and easy to implement, this topology suffers from the lack of effective utilization of the stored ultracapacitor energy, thereby reducing its volumetric efficiency.

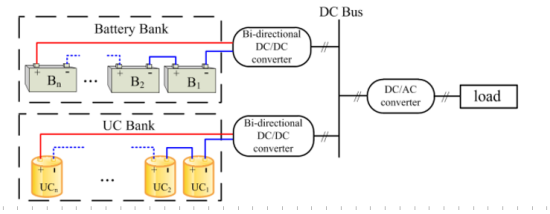

Figure 2.9: Active HESS Configuration

2.5.2 Active HESS Configuration

For better utilization of battery and ultracapacitors in HESS, power electronic converters are usually employed for interfacing them with the DC bus. In active HESS configuration (Figure 2.10), both the battery and UC are interfaced to the DC-link with the help of dc-dc converters. The active control of these two components enhances the overall system performance and flexibility. It is also expected to bring about a considerable improvement in the life cycle of the battery. There are two types of active HESS configurations namely parallel active and cascaded configuration [12], [19]. Figure 2.9 depicts the parallel active HESS configuration in which both the battery and UC are isolated from the DC-link. In cascaded configuration , the battery side converter is usually current controlled for prevention against high charging and discharging currents, while the UC side converter is voltage controlled for the smooth regulation of dc link voltage. The power losses in this configuration are usually high due to the large voltage swings in between ultracapacitor and the dc-link on account of wider operational voltage variations of the UC.

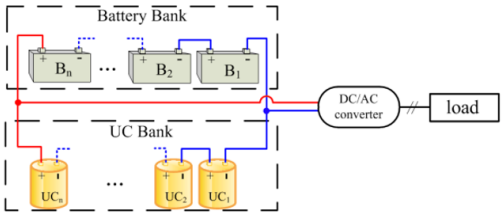

Figure 2.10: Active HESS Configuration

2.5.3 Semi-active HESS Configuration

The semi-active configuration is a slight variation of active configuration where either of the two power electronic converters is usually eliminated to reduce the overall space and size of the ESS. In battery semi-active HESS configuration Figure 2.11.a, the UC is connected across the DC-link without any power electronic converter while the battery is interfaced to the UC with the aid of a bidirectional converter. This arrangement allows improvement in the control of battery current irrespective of the fluctuation in load demand. Furthermore, the appropriate sizing of battery pack can be achieved as the battery voltage is not required to be same as that of the DCbus voltage. Nevertheless, the linear charge/discharge characteristics of the UC causes sharp fluctuations in the DC-link voltage resulting in reduced system

performance. Thus, to stabilize the dc-link voltage, ultracapacitors with higher capacity are required and hence the cost of the system is subsequently increased. Figure 2.11.b depicts the UC semi-active configuration where the ultracapacitor and the battery are interfaced by means of a bi-directional dc-dc converter while the battery is connected directly across the dc-link. Thus, a stable DC voltage can be obtained in this configuration. This topological connection also facilitates in the improvement of the volumetric efficiency of the ultracapacitors.

[b]0.45

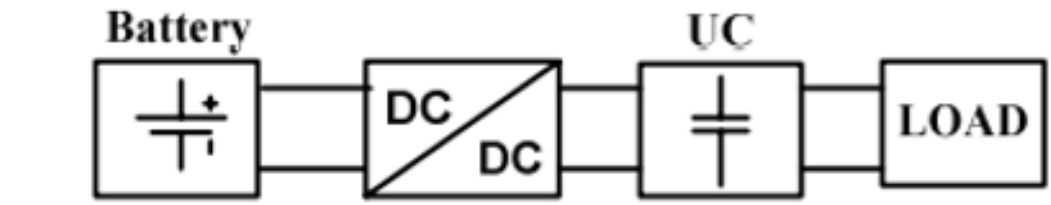

(a)

[b]0.45

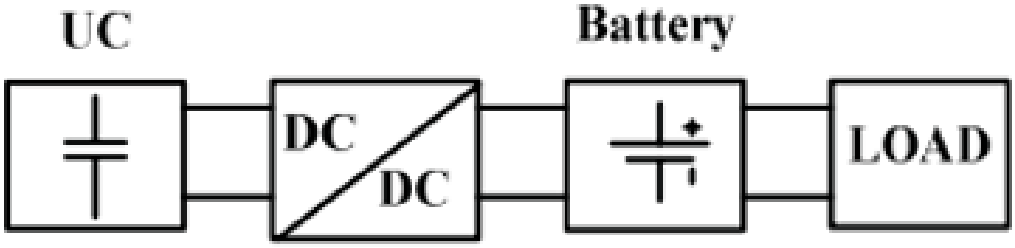

(b)

Figure 2.11: (a) Battery semi-active HESS configuration and (b) UC semi-active HESS configuration

Chapter 3

Model of Supercapacitors

3.1 Simplified Equivalent Circuit Models for Supercapacitors

Supercapacitors are complex devices, so we need to make simple models to understand how they work. There are two main types of models: physics-based and equivalent circuit. We will focus on equivalent circuit models because they are easier to use and can still give us accurate results. Equivalent circuit models are like simplified versions of the real supercapacitor. They don't show all the details of the chemical reactions inside the cell, but they can still tell us how the cell will behave when we charge or discharge it. A good equivalent circuit model should be Accurate enough to represent a real supercapacitor, especially in the short term. It simple enough to be used in real-time simulations. it should be suitable for the time scales we are interested in, which are usually seconds to minutes

3.2 Equivalent Circuit Modelling of supercapacitors

The equivalent circuit model (ECM) of a SC, which is an easy, simple, and accurate method in contrast to the other models such as electrochemical models, which require high computational complexity [17]. Additionally, the ECM can also be used as an important tool to reveal the nonlinear behavior of charging and discharging in SCs, as well as the redistribution of charges and self-discharge processes before deploying SCs in practical applications. In the literature, various ECMs for SCs have been

developed recently. The reported ECMs differ in representing the implementation of SCs in different applications, and for specific applications, specific ECMs are proposed. In some reports of modeling SCs through ECM and analyses in the time or frequency domain , diverse resistive-capacitive (RC) networks are used. In the last work published by this group [7], several ECMs for SCs reported in the literature were reviewed. In this paper, we now refer to the ECMs that have been published in recent years. In this chapter, some of the most famous models of supercapacitors are introduced. The modeling of the component is addressed from different points of view, starting from the molecular aspect up to what concerns its most macroscopic behavior. The latter is the one on which the thesis will be focused and therefore models that develop the molecular aspect of the component will not be considered. In literature, several models for supercapacitors are introduced, from which four models have been identified for the purpose of this work. These are:

- The RC series model
- The Two-Branch model
- The Zubieta model
- The Series model
- Transmission line network Model
- RC ladder network model

Note that the value of the capacitance of the models may generally depend on the voltage. This aspect is fundamental to a better representation of the behavior of the supercapacitor cell. In fact, the capacitance value tends to vary as voltage varies. Except for the RC model, which only gives a simplified representation of the component's behavior, the other models are more accurate because they present a breakdown of the time constant within a cell, dividing its representation into several branches.

3.3 Simple Model of a Supercapacitor

The simplest ultracapacitor circuit model RC model, which has only one RC branch. Figure 3.1 is the ultracapacitor simple RC model. This model is composed of a resistor R, which models the ultracapacitor's ohomic loss, usually called equivalent

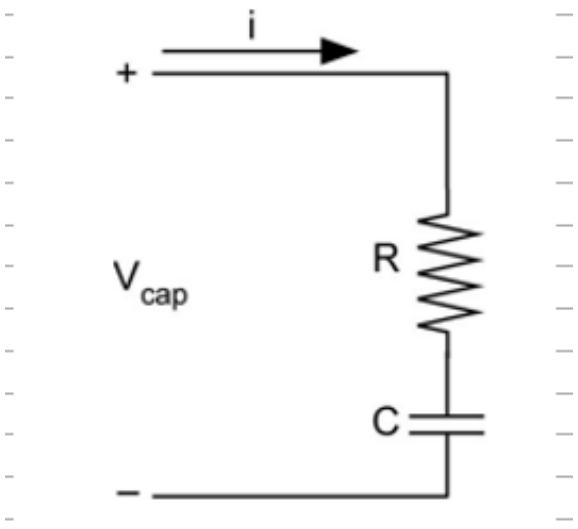

Figure 3.1: Classical Model

series resistor (ESR) and a capacitor C, which simulate the ultracapacitor's capacitance during charging and discharging effects[22] The RC series model only introduce one time constant governing the dynamic of the cell which is simply given by the product of the resistance and the capacitance of the cell.

Capacitor behavior can be described by a mathematical equation as shown below :

$$V_C(t) = V_C(0) - \int_0^t \frac{(I_{Scout}(t) + I_{Leakage}) \cdot t}{C}\, dt \tag{3.1}$$

Vc(0) : is the initial voltage of the capacitor

$$V_{Scout}(t) = V_C(t) - I_{Scout}(t) \cdot R_{ESR} \tag{3.2}$$

This model is used to have a general overview of the component's behavior. It should be noted that this model does not consider the self-discharge phenomenon as there is only one resistance in the model. This is one of the disadvantages of this model. It also cannot accurately represent 2.1.1 The RC series model Figure 3.1 RC model 26 charging and discharging cycles with accuracy.[4] In the latter there are voltage variations increasing and decreasing of the voltage that cannot be adequately represented with this model. On the other hand, however, this model has a great advantage which is its simplicity

3.4 Two-Branch Model of a Supercapacitor

This model is more complex than the previous one. In fact, the Two Branch model, shown in Figure 3.2, is a model in which a subdivision of the time constant takes place [25]. The circuit consists of several branches in which the representation of the component dynamics is divided. Note that the first branch is composed of a resistance and a variable capacitor. This capacitor is the sum of two terms: a constant one and a voltage dependent one. The capacitance of this branch is the main accumulation component while the resistance of this branch is the one that acts as Equivalent Series Resistance (ESR).

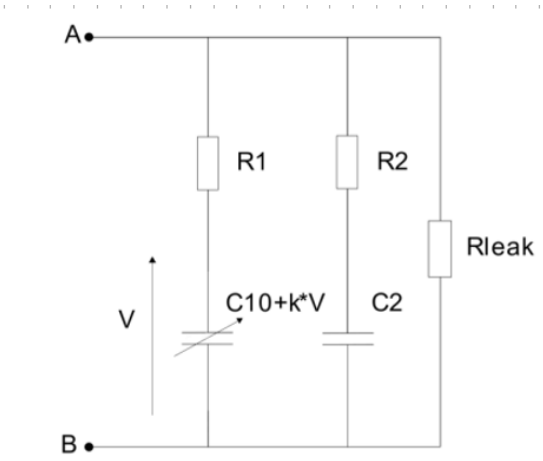

Figure 3.2: Two-branch model

This branch is the one with the fastest dynamics. The second branch represents the medium-long term and is in the order of magnitude of minutes. The second branch does not contain variable terms. The third and final branch is that which represents the phenomenon of self-discharge. This term is actually relevant for the complete representation of the component. However, this model is used for representations of a generally shorter period and, as in the case in question, it will not be considered. In this work, we simplify this model by eliminating the third branch and obtaining the model of Figure 3.3. Increasing capacitor as voltage increases means that the stored energy also increases.

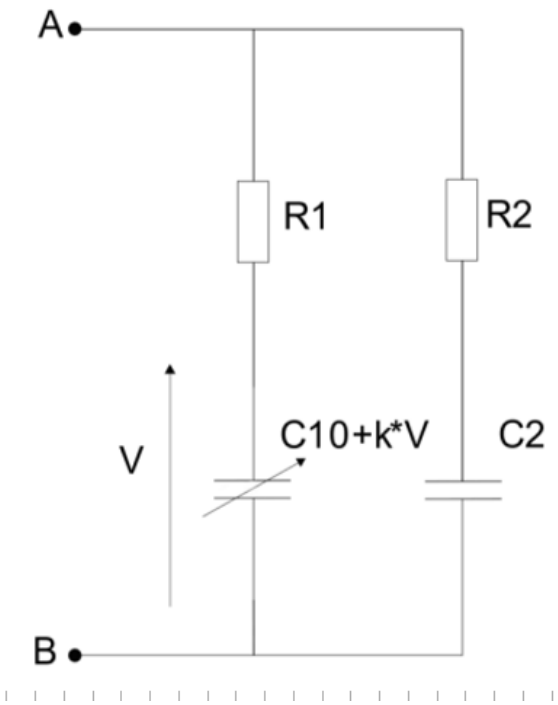

Figure 3.3: Simplified two-branch model

3.5 The Zubieta Model

The Three Branch Model introduced in [26], includes three series RC branches in parallel, where the three RC branches are termed the immediate branch, delayed branch, and long-term branch, along with a leakage resistor, as shown in figure 3.4

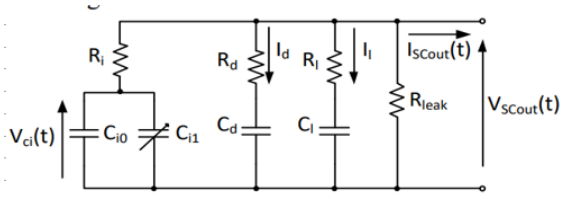

Figure 3.4: Three Branch Model

The immediate branch, which includes Ri, Ci0 and a voltage-dependent capacitor Ci1, is used to describe the immediate behavior of the SC in the time range of seconds. The voltage-dependent capacitor is expressed as:

$$C_{i1}(V_{ci}) = k_v \cdot V_{ci} \tag{3.3}$$

The voltage-dependent capacitor models the nonlinear characteristics of a SC. The delayed branch with Rd and Cd is used to describe the SC behavior in the time range of minutes. The long-term branch of Rl and Cl, determines the behavior for times longer than 10 minutes. The leakage resistor Rleak employed to describe the self-discharge phenomenon in time range of hours.

Due to the variable capacitance model and multi time range RC branches, the Three Branch Model can adequately represent the SC internal charge redistribution characteristic and has a high accuracy when voltages above 40 % of the rated voltage. However, the error at low voltages may over 10% of the rated voltage caused by the simplified model and parameter identification process.

3.6 Transmission Line Network Model of a Supercapacitor

The SC can be represented by a transmission line model with voltage dependent distributed capacitance [5]. The transmission line model indicates that the capacitance increases as the voltage increases and a time dependent apparent capacitance is introduced due to the space distribution of electrical charge and electrostatic energy. The transmission line model under a step current with magnitude of I is shown in Figure 3.5, where x represents for the distance. Compared to the three-branch model, the transmission line model causes a difference in stored or delivered charge of the SC, which depends on the current level for a certain voltage variation. Less deliverable charge and deliverable energy storage can be obtained in the transmission line model, where the difference is over 18% [27]. Although the model has a higher accuracy, the identification procedure and development of the analytical model based on the transmission line model is complex, thus the transmission line model is not widely used in SC simulation.

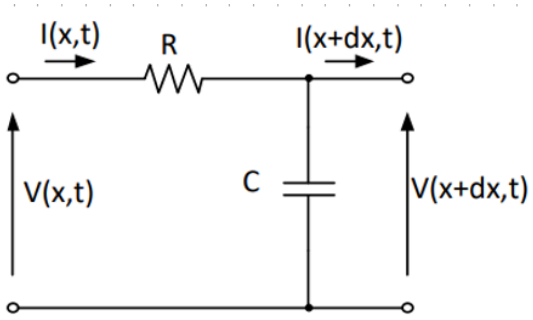

Figure 3.5: Transmission Line model

3.7 The SC Ladder Model

The SC multi-stage ladder model, rooted in impedance spectroscopic measurement, builds upon Miller's five-stage ladder model depicted in Figure 3.6, offering accurate frequency analysis up to 10 kHz. Despite its precision in capturing frequency dynamics, the high-order step time limitations render the ladder model inefficient in simulations. To address this, an automated order selection method, based on the five-stage ladder model, has been devised for fitting diverse frequency bands in simulations . Each order model corresponds to distinct frequency ranges, allowing the justification of the ladder network's correct order. This optimization ensures an optimal solution, minimizing calculation errors, and conserving computational time in line with the required simulation time step. The parameter values of the reduced order model are derived from the five-stage ladder model, maintaining accuracy while streamlining the simulation process. Despite the improved accuracy and simulation performance of the automatic order selection multi-stage ladder model, its parameter identification mirrors the complexity of the five-stage ladder model, necessitating a comprehensive electrochemical impedance spectroscopy (EIS) method for the identification process. Furthermore, the impedance response of the automatic order selection multi-stage ladder model may differ for various types of supercapacitors under distinct operating conditions. This variation prompts adjustments in the order number to effectively accommodate the complete frequency range, ensuring adaptability across diverse scenarios.

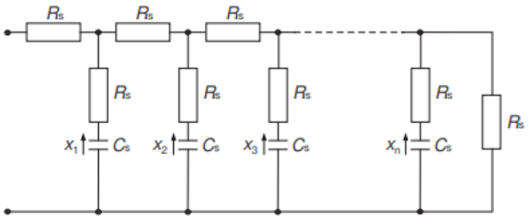

Figure 3.6: Electrical Cicuit Model of a supercapacitor

Chapter 4

Model Validation And Simulation Results

In this section, we delve into the specifications and characteristics of supercapacitor cells, providing a comprehensive overview of their development and implementation. We discuss the various product specifications that define the performance and efficiency of supercapacitors, including their capacity, voltage range, and energy density. Furthermore, we explore the process of developing equivalent circuit models, which simplify the complex inner workings of supercapacitors. These models are crucial for predicting cell behavior during charging and discharging phases, facilitating real-time simulations and practical applications in various time scales, typically ranging from seconds to minutes.

4.1 Supercapacitor Cell

The Supercapacitor Cell that is considered below is extracted from Maxwell Technologies directly from the datasheet provided by the manufacturer.

TABLE () PRODUCT SPECIFICATIONS & CHARACTERISTICS	
ELECTRICAL	Bcap3000 p270 k04
Rated Voltage (V_R)	2.7 V
Surge Voltage (V_{surge})	2.85 V
Rated Capacitance (C_R)	3250 F
Equivalent Series Resistance (ESR_{DC})	0.15 mΩ
Leakage Current (I_{LEAK})	2.8 mA
Peak Current (I_{peak})	2300 A
Continuous Current (I_{max}) at ΔT = 15°C	170 A
Continuous Current (I_{max}) at ΔT = 40°C	280 A
LIFE	
High Temperature Life(t_{65C}) at V_R=2.7 V	3000 hours
Projected Life Time (t_{25C}) at V_R=2.7 V	10 years
Projected Cycle Life (n_{CYCLE})	1,000,000 cycles
Shelf Life (t_{SHELF}) Stored uncharged, TA < 25°C and RH < 50%	4 years

POWER & ENERGY	
Usable Specific Power (P_d)	12.3 Kw/kg
Impedance Match Specific Power (P_{MAX})	25.6 Kw/kg
Gravimetric Specific Energy (E_d)	6.9 Kw/kg
Stored Energy (E_{MAX})	3.3 Wh
TEMPERATURE & THERMAL	
Operating Temperature	25 °C
Storage Temperature (T_{STG})	Min =-40 °C max= 70 °C
Thermal Resistance (R_{th})	2.1 °C/W
Thermal Capacitance	520 J/°C
PHYSICAL	
Mass (m)	476 g
Recommended Torque on Threaded Connector	12 Nm
Recommended Welding on Jove Terminal (K05)	-
Vibration	ISO 16750-3
Shock	IEC 60068-2-27
SAFETY	
Certifications	UL810A, RoHS, REACH

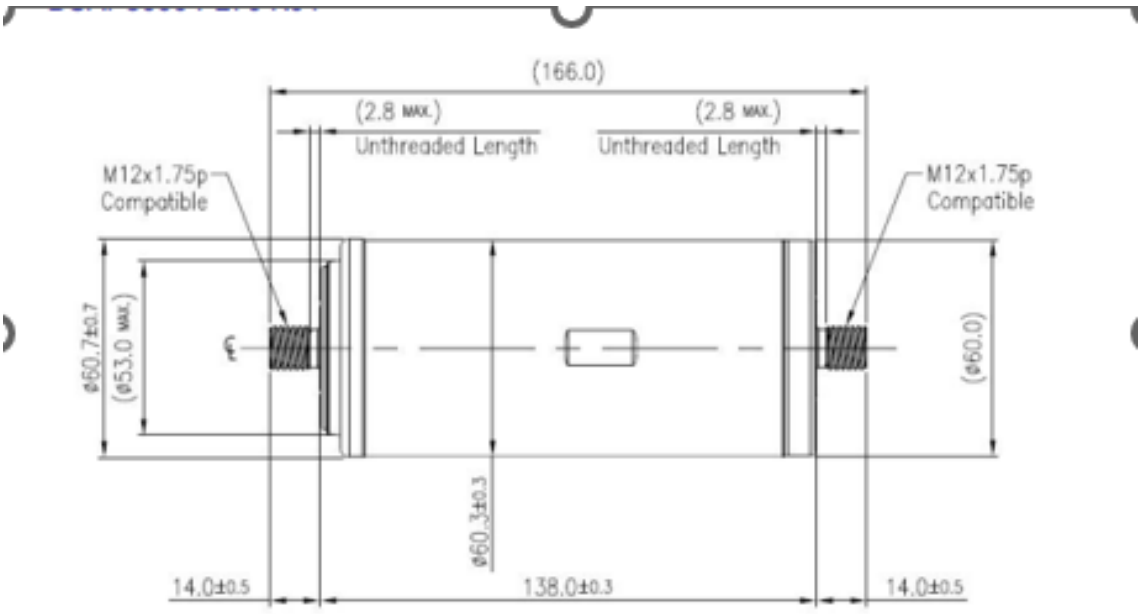

Figure 4.1: Cell structure from data-sheet.(Bcap3000 p270 k04) Courtesy of picture: Maxwell Technologies

4.2 Development and Implementation of Multi-Branch Equivalent Circuit Models for Supercapacitors Using PLECS: Architecture, Simulation, and Analysis

4.2.1 Overview

The use of SCs in real-time applications in electronic circuits requires a circuit model to correctly predict their behavior. For rough sizing in power systems, a linear representation with an 3RC circuit may be sufficient. The purpose of this model is to calculate ultracapacitor's SOC and working voltage according to the original open-circuit voltage and demand current of ultracapacitor.it is essential that the method is capable of applying large DC current signals across an Ultracapacitor at low rated voltage. Charging/Discharging method is one of the most suitable ways for this application as the above can be achieved in this method. For measuring Capacitance of UC by charging/ discharging method, time taken to charge from lower preset voltage to higher preset voltage or discharge from higher preset voltage to lower

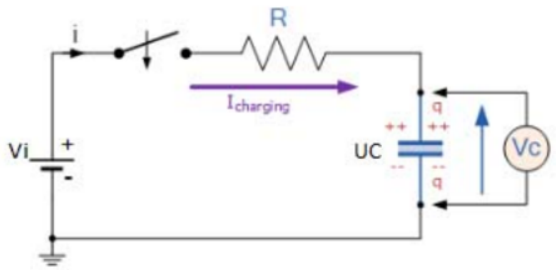

Figure 4.2: Charging Cicuit of UC

preset voltage, is determined. From this, Capacitance C of Ultracapacitor can be arrived using formulae described below. In addition. To understand charging/ discharging circuit and to arrive at formulae for Capacitance C, let us consider a simple charging circuit as given in Figure 1 below, having a power supply with voltage Vi, a Switch, a Resistance R and an Ultracapacitor. Voltage across UC is VC. Let t1 be the time taken for the Ultracapacitor to get charged to voltage level V1 and t2 be the time taken to get charged to Voltage level V2. The voltage across the ultracapacitor at time t1 is given by

$$V_1 = V_i \left(1 - e^{-t_1/RC}\right) \tag{4.1}$$

Where Vi is the supply voltage and RC is the time constant of the charging circuit. Similarly, the voltage across the ultracapacitor at time t2 is given by

$$V_2 = V_i \left(1 - e^{-t_2/RC}\right) \tag{4.2}$$

From the above equations (1) and (2), the calculations for arriving at Capacitance of Ultracapacitor during charging cycle are given in the following equations:

$$\frac{t_1}{RC} = -\ln\left(1 - \frac{V_1}{V_i}\right) \tag{4.3}$$

$$\frac{t_2}{RC} = -\ln\left(1 - \frac{V_2}{V_i}\right) \tag{4.4}$$

In the above equation, t2-t1 is the pulse width measured in seconds through the circuit. The above concept has been implemented for measurement of capacitance using Charge/Discharge circuit.
Considering the Multi-branch Model, the following data are needed in order to implement the circuit:

- Coefficient k_v
- Resistance R_1
- Capacitance C_1
- Resistance R_2
- Capacitance C_2
- Resistance R_3
- Capacitance C_3
- Resistance R_4
- Maximum Voltage V_{rated}
- Initial Voltage

4.2.2 Block diagram of the Multi-branch circuit

Simulation and Analysis of Supercapacitor Dynamics Using Multi-Branch Equivalent Circuit Models in PLECS

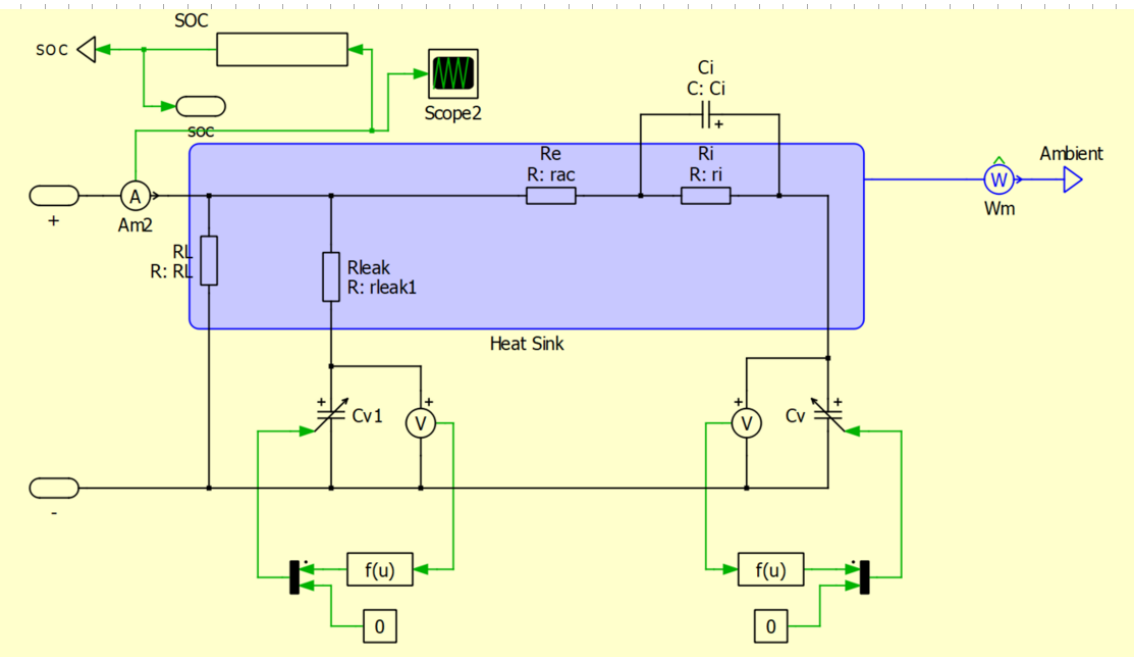

Figure 4.3: Multi-branch structure of Supercap including thermal condition

- **Thermal Behavior of a Supercapacitor under Operating Condition**

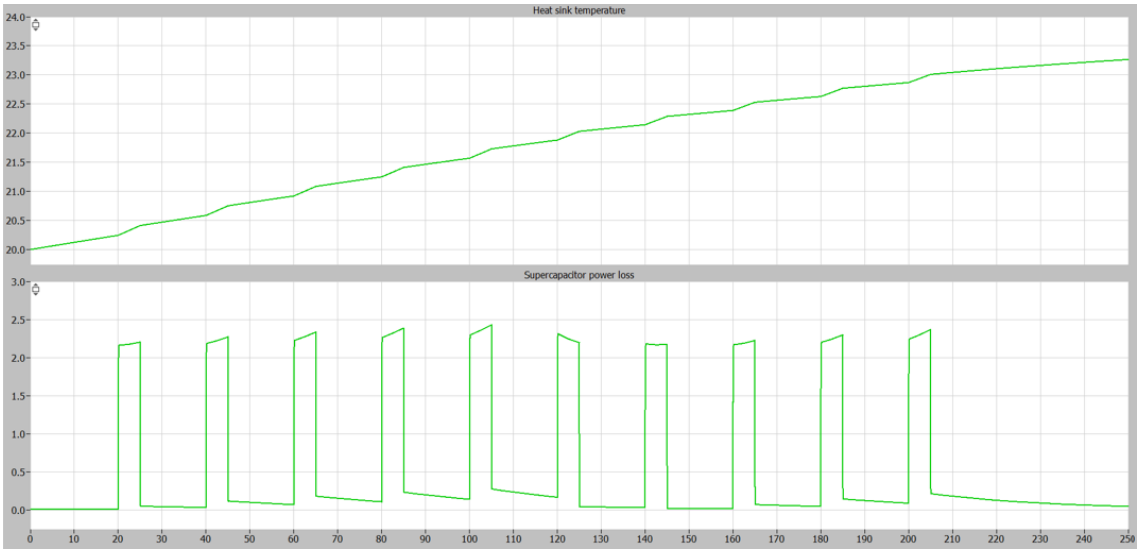

Figure 4.4: Heat sink temperature and Supercapacitor Power loss

The provided plots illustrate the dynamic thermal behavior of a supercapacitor under repetitive charging and discharging cycles. The periodic power losses due to resistive heating cause the heat sink temperature to rise gradually, emphasizing the importance of thermal management in supercapacitor applications to ensure system reliability and efficiency.

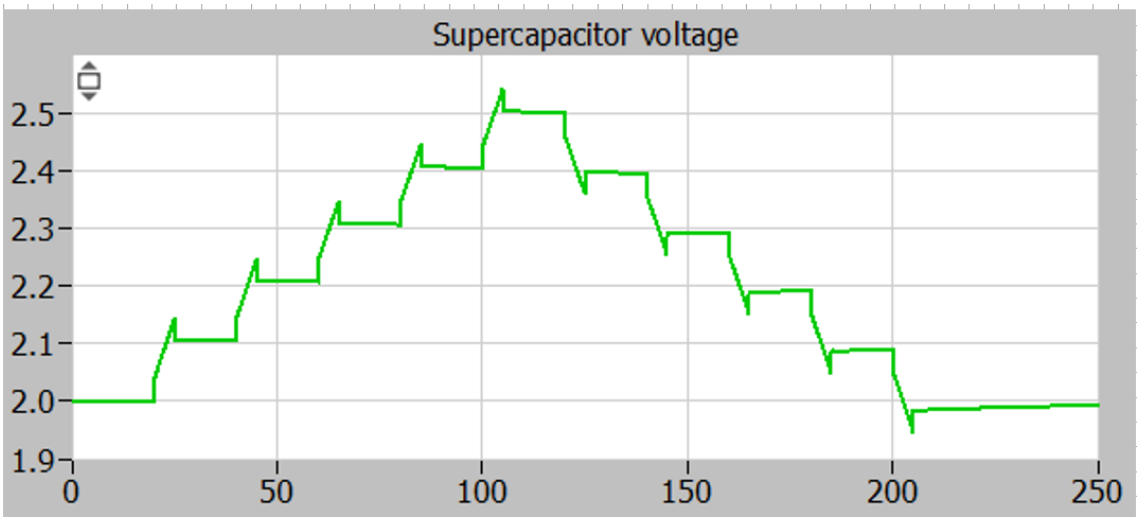

Figure 4.5: Voltage trend under repetitive charging and discharging

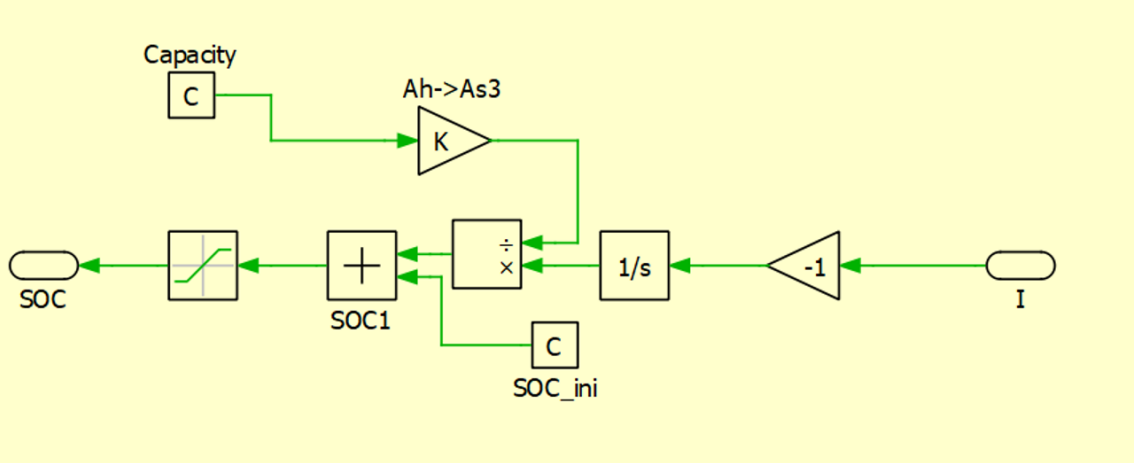

Figure 4.6: Represents a State of Charge (SOC) model

The SOC model accurately tracks the state of charge of a supercapacitor by integrating the current over time, adjusting for initial charge, and normalizing by the total capacity. It is crucial for applications requiring precise energy management and monitoring in supercapacitors.

- **I (Current Source)**: Represents the current flowing into or out of the supercapacitor.
- **-1 (Inverter)**: Inverts the current direction, essential for correct SOC calculation depending on whether the supercapacitor is charging or discharging.
- **1/s (Integrator)**: Integrates the current over time to calculate the charge (or discharge) amount. This is a key part of determining the SOC.
- **Division Block**: Divides the integrated current by the capacity of the supercapacitor (Ah to As conversion), giving the charge as a fraction of the total capacity.
- **SOC_init (Initial SOC)**: Represents the initial state of charge of the supercapacitor.
- **Addition Block (SOC1)**: Adds the initial SOC to the calculated charge/discharge fraction to obtain the current SOC.
- **SOC Block**: Outputs the SOC value, which can be used for monitoring and further analysis.

- **Capacity (C)**: Represents the total charge capacity of the supercapacitor.

- **K (Gain/Conversion Factor)**: Converts the capacity from ampere-hours (Ah) to ampere-seconds (As), aligning with the current integration units.

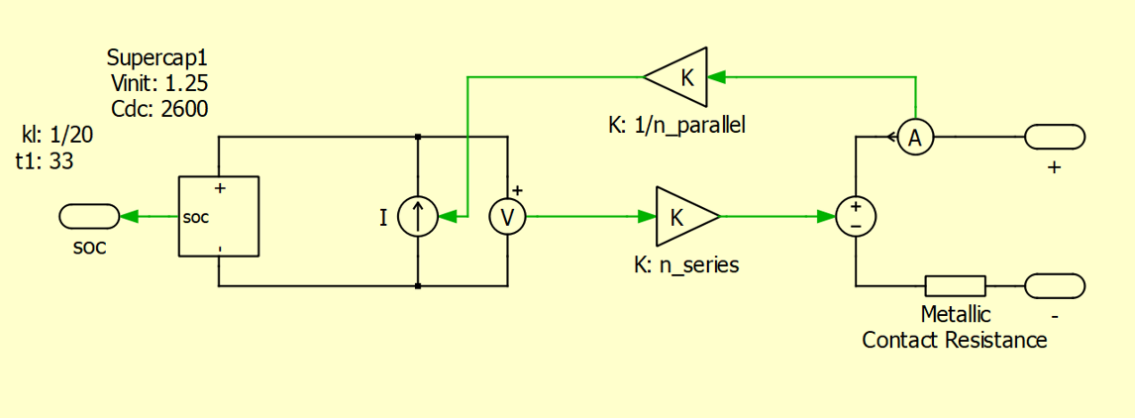

Figure 4.7: Configuration of supercapacitors in both series and parallel

The model includes specific blocks to scale the current and voltage, representing the series and parallel configurations of supercapacitors. The "K: 1/n_parallel" block scales the current for parallel branches, and the "K: n_series" block scales the voltage for series connections. This allows the model to simulate the behavior of supercapacitor modules accurately, reflecting how they would perform in practical applications with series and parallel configurations.

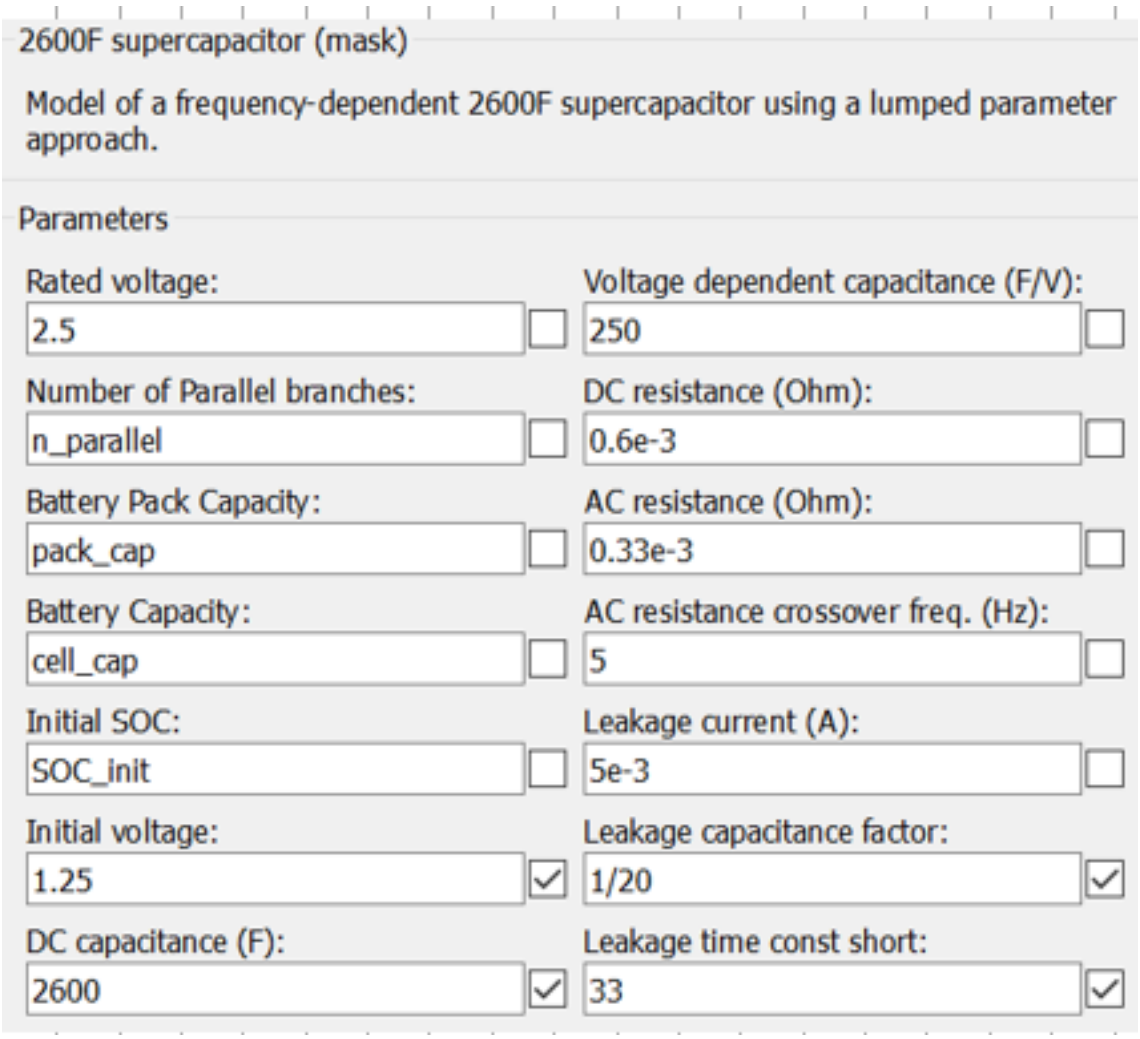

Figure 4.8: Parameters related to the supercapacitor model

4.2.3 GaN FET as Switches

4.2.3.1 Introduction

Wide-bandgap materials are increasingly replacing silicon in various power electronics applications. Currently, gallium nitride (GaN) stands out as a leading technology in this field, enabling the creation of devices with higher power density, lower on-resistance, and extremely high-frequency switching capabilities [18] . The wide bandgap characteristic of GaN results in a high critical electric field, allowing for the design of electronic devices with a shorter drift region and, consequently, lower on-state resistance compared to silicon-based devices with the same voltage rating.

However, the high switching speed of GaN power devices necessitates careful power loop layout design in converter applications.

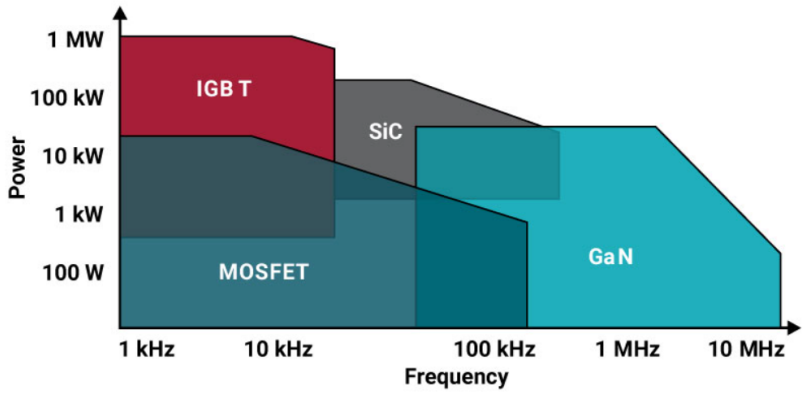

Figure 4.9: GaN FET used as a switch in power electronics.

The figure 4.9 clearly demonstrates that GaN FETs (Gallium Nitride Field-Effect Transistors) operate effectively at much higher frequencies compared to traditional silicon-based technologies like MOSFETs and IGBTs. GaN technology excels particularly in the frequency range above 100 kHz, extending up to 10 MHz, making it ideal for high-frequency switching applications where efficiency and power density are critical.

4.2.3.2 Structure of GaN FET

Transistors utilizing GaN technology are lateral power devices within the field-effect transistor (FET) category, featuring a current conduction channel between the drain and source terminals [20]. The conduction current is controlled by modulating the gate voltage. Like other FET devices, GaN FETs naturally operate in depletion mode, making the simplest form of a GaN FET a normally-on switch. A simplified structure of a depletion-mode GaN FET is depicted in Figure 4.10. Typically, the gate electrode is created using a Schottky contact on the surface of the layer. Applying a negative voltage to this electrode relative to the source polarizes the Schottky barrier in reverse, switching the device to the OFF state. Figure 4.10 also illustrates the two-dimensional electron gas (2DEG) formed in the AlGaN/GaN heterojunction. However, to enhance the competitiveness of GaN power transistors with SiC and Si-based GaN FETs, designers have developed normally-off structures for HEMT power electronics switches.

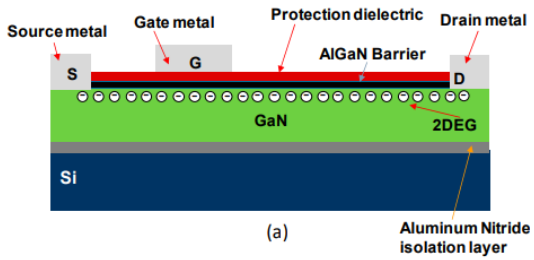

Figure 4.10: Normally on GaN (d-mode)

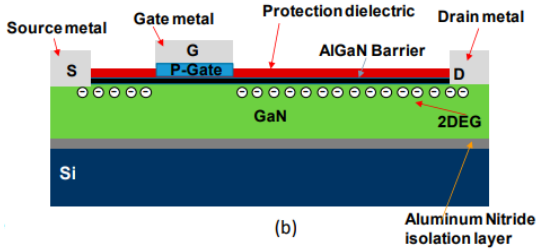

Figure 4.11: Normally off GaN (e-mode)

In Figure 4.10, the creation of a two-dimensional electron gas (2DEG) at the AlGaN/GaN heterojunction is illustrated. To enhance the competitiveness of GaN-based HEMTs (High Electron Mobility Transistors) against SiC and traditional Si-based devices, designers have developed typically off structures for GaN power transistors, making them more suitable for power electronics switching applications.

In Figure 4.11, the device is shown in its off-state. In this configuration, the p-type GaN gate layer is grown atop the AlGaN barrier, effectively depleting the two-dimensional electron gas (2DEG) when the gate-source voltage (V_{GS}) is zero, ensuring a normally off state. When a positive voltage exceeding the threshold is applied, the 2DEG is restored. However, if the gate voltage is below the threshold, the device behaves like a diode, allowing reverse conduction without reverse recovery charge (Q_{rr}).

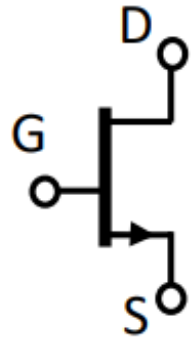

Figure 4.12: Normally on GaN (d-mode)

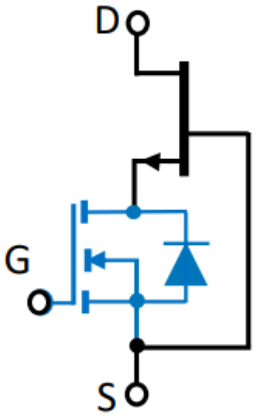

Figure 4.13: Normally off Cascode GaN (d-mode)

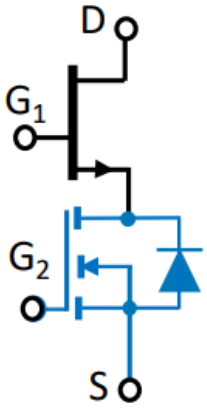

Figure 4.14: Direct drive GaN (d-mode)

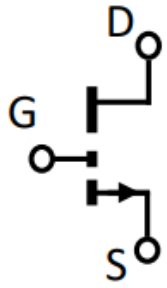

Figure 4.15: Normally off GaN (e-mode)

The normally on GaN transistor depicted in Figure 4.12 operates in depletion mode (d-mode), meaning it remains on when the gate voltage (VGS) is at 0V and turns off with a VGS of -15V. This structure is known for its simplicity and low on-resistance (RDSon), but it is not typically used alone as a power switch. Instead, it is integrated into a cascode configuration as shown in Figure 4.13, where a low-voltage MOSFET is added in series with the GaN transistor. This setup combines the efficient switching of GaN with the familiar gate-driving characteristics of the MOSFET. The cascode structure effectively creates a normally off switch, ideal for low-voltage applications, by leveraging the bidirectional nature of the d-mode GaN and the MOSFET's gate control for smooth switching transitions.

The critical issues of the cascode arrangement are related to the following points:

- The complexity of the package solution;
- The increase in the stray inductances in the power loop;
- The presence of the reverse recovery of the MOSFET body diode;
- The quasi-uncontrolled GaN switching due to a lack of control drive of the HEMT gate.

Figure 4.14 illustrates a direct-drive GaN power transistor configuration, which modifies the standard cascode setup. In this arrangement, the d-mode GaN gate is not connected to the low-voltage MOSFET source, allowing direct control with a negative unipolar voltage (-15V, 0V). This setup uses the MOSFET as a protective device to prevent series shoot-through. The direct-drive approach enhances the use of the GaN FET's switching properties while minimizing uncontrolled commutation, though it increases stray inductances and requires four device pins due to the two available gates.

The enhancement-mode (e-mode) GaN power transistor, shown in Figure 4.15, is created by modifying the gate structure of a depletion-mode device to positively shift the threshold voltage, forming a conductive channel. Similar to an enhancement-mode MOSFET, the e-mode GaN FET requires a gate voltage of 0V to +6V to operate. However, it has higher reverse conduction losses during dead times due to an equivalent diode conduction mechanism. E-mode GaN transistors are currently the most widely used and are the focus of ongoing optimization efforts, especially for high-voltage applications.

4.2.3.3 GaN in Power Electronics Applications

E-mode GaN FETs are increasingly utilized in power electronics due to their superior performance over traditional silicon MOSFETs, particularly in low-voltage applications where they contribute to more compact and efficient designs. Their ability to operate at high switching frequencies makes them ideal for specialized applications, although their higher cost remains a limitation to broader adoption. In high-voltage systems, GaN FETs are selectively used, especially in areas like automotive battery chargers and photovoltaic inverters, where their advantages in energy conversion are being actively explored. Comparisons with other technologies, like SiC MOSFETs and silicon super-junction MOSFETs, highlight GaN FETs' strengths and potential, particularly in applications requiring high efficiency and compact size. As research continues, GaN FETs are expected to play a growing role in power electronics, contributing significantly to advancements in energy conversion technologies.

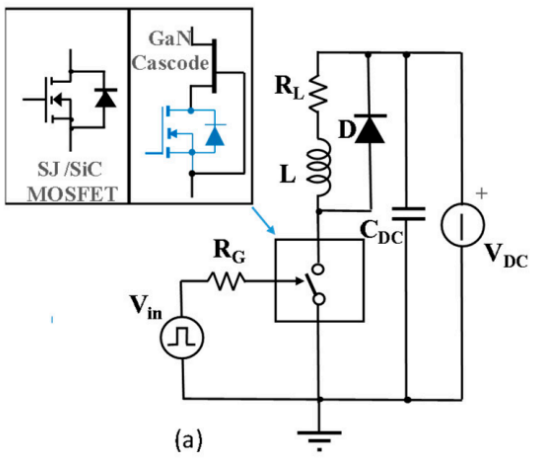

Figure 4.16: Inductive-load-switching test circuit

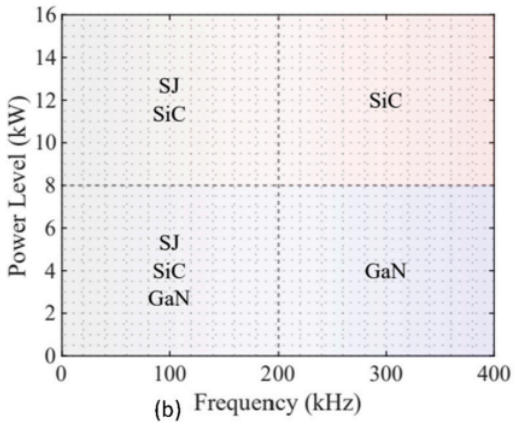

Figure 4.17: Application areas trend for SiC, SJ, and GaN technologies

Figure 4.16 presents a comparison of power losses among different types of transistors, including SiC MOSFETs, silicon super-junction (SJ) MOSFETs, and GaN FETs configured in a d-mode cascode setup. The comparison is conducted at a 400V DC bus with varying load current amplitudes during inductive switching. The data highlights the specific conditions under which each technology performs best, providing insights into their relative efficiency and suitability for different power electronics applications.

Figure 4.17 visually demonstrates the optimal application areas for each tested transistor technology, based on the switching frequency and corresponding power losses. It clearly delineates where GaN FETs, SiC MOSFETs, and SJ MOSFETs excel, particularly showing that GaN FETs are more effective in high-frequency switching environments. This helps define the niche areas where GaN transistors outperform their silicon-based counterparts, particularly in high-efficiency, high-frequency applications.

4.2.4 DC-DC Boost Converter & DC-DC buck Converter Models

4.2.4.1 Architecture of DC-DC Boost Converter

The DC-DC Boost converter is responsible for discharging the supercapacitor.

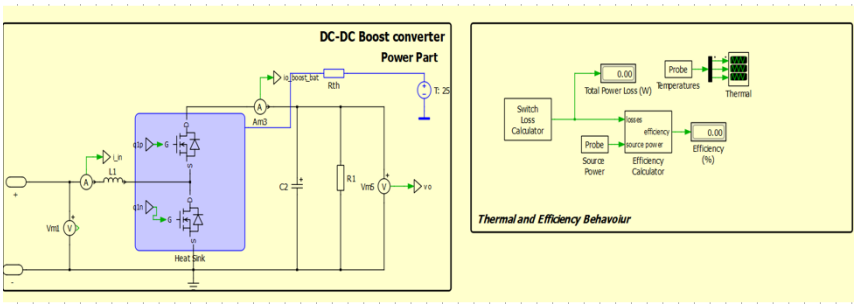

Figure 4.18: Power part of DC-DC Boost Converter Closed Loop.

The DC-DC Boost Converter model shown in Figure 4.18 operates by stepping up the input DC voltage to a higher output DC voltage using key components such as an inductor, a switching transistor (MOSFET), a diode, and a capacitor. The power conversion process is based on two distinct phases: the energy storage phase and the energy transfer phase. During the energy storage phase, the switch is turned on, creating a closed path between the input voltage source and the inductor, allowing the inductor to store energy in the form of a magnetic field. In this phase, the diode is reverse-biased, preventing current flow to the output. In the energy transfer phase, the switch is turned off, causing the inductor to release its stored energy. This reverses the inductor's polarity, adding to the input voltage and boosting the overall output voltage. During this phase, the diode becomes forward-biased, allowing the current to flow to the load and charging the output capacitor, which smooths the output voltage. By controlling the switching duty cycle, the output voltage is regulated at a higher level than the input voltage.
In addition to the power conversion, the model includes a thermal and efficiency behavior section to simulate real-world losses due to inefficiencies in switching components, such as the MOSFET and the diode. The thermal behavior is primarily modeled through the Switch Loss Calculator, which accounts for conduction losses when the MOSFET is on, and switching losses during the transitions between on and off states. These losses, along with the diode's forward voltage drop, are major sources of heat generation and affect the overall system performance. The thermal probes in the model track these losses and calculate the temperature rise

due to heat dissipation. The efficiency of the system is calculated by comparing the output power delivered to the load with the input power drawn from the source. This efficiency is typically reduced by the power lost as heat in the switching and conduction processes. Overall, this model provides both a voltage boost through power conversion and a realistic representation of thermal behavior and efficiency to better understand the performance of the DC-DC Boost Converter under real operating conditions.

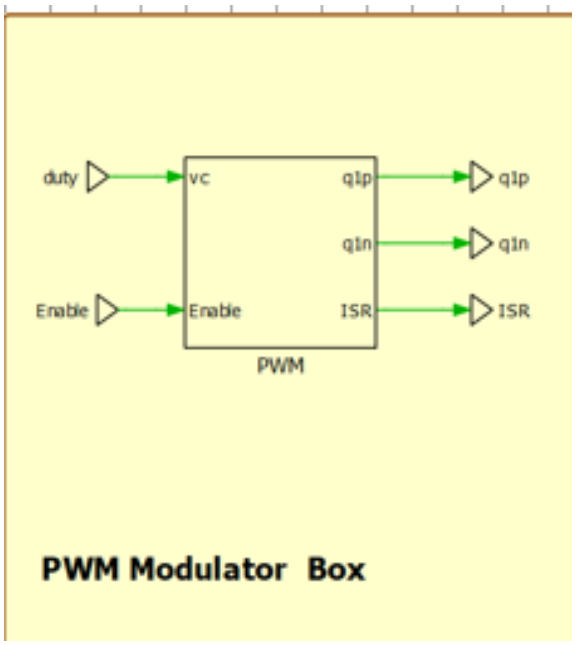

Figure 4.19: PWM Modulator

Figure 4.19 depicts a PWM (Pulse Width Modulation) Modulator Box, which is used in power electronics to generate control signals for switches (such as transistors) in a DC-DC converter. This block is essential for controlling the switching behavior of the power circuit, which directly affects the output voltage and efficiency of the system. As shown in Figure 4.20, the parameters are used for regulating the switching frequency.

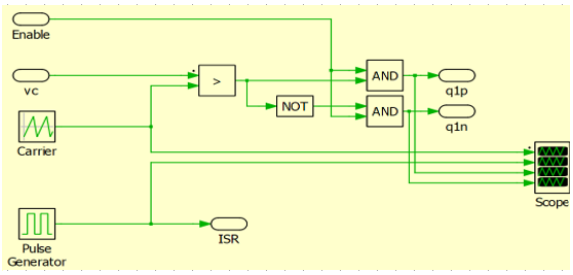

Figure 4.20: PWM Modulator Parameters

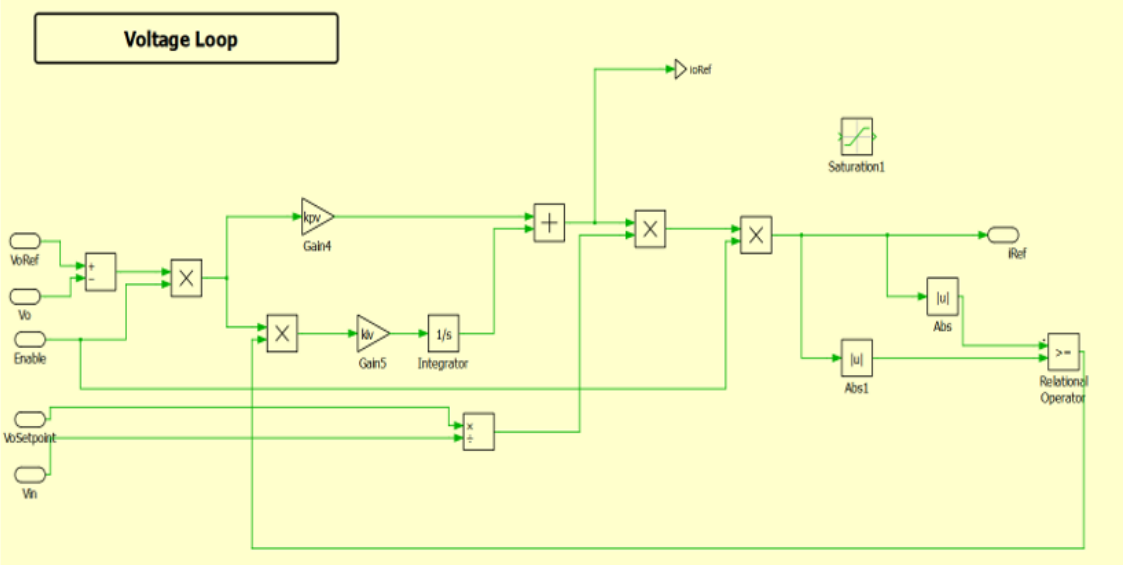

Figure 4.21: Voltage Loop Block Diagram

The Voltage Loop control system, represented in Figure 4.21, is typically used in DC-DC converters to regulate the output voltage. This loop ensures that the output voltage stays at the desired level (reference voltage) by continuously adjusting the control signals based on feedback from the actual output voltage.
The Voltage Loop control system regulates the output voltage of a DC-DC converter by continuously monitoring the actual output voltage and comparing it with a reference value. If the actual voltage deviates from the reference, an error signal is generated. This error is processed by a Proportional-Integral (PI) controller, which adjusts the converter's control signals, ultimately modifying the current that flows to the output.

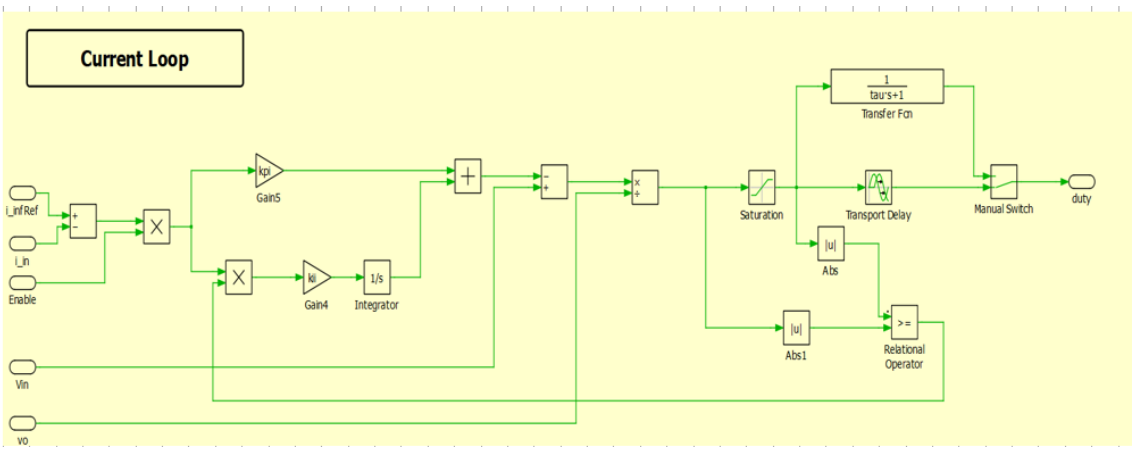

Figure 4.22: Current Loop Block Diagram

Figure 4.22 illustrates a Current Loop Control System commonly used in DC-DC converters to regulate the circuit's current. This system dynamically adjusts the duty cycle of the switching transistors based on real-time feedback from the measured current, ensuring it remains within the desired range. The loop continuously compares the actual current to a reference value, and any deviation is corrected by a Proportional-Integral (PI) Controller, which modifies the duty cycle of the switching transistor accordingly. Supporting components like the Saturation, Transfer Function, and Transport Delay blocks maintain system stability and ensure safe response times. The Manual Switch provides control flexibility, while the Relational Operator enforces predefined current limits, making this current loop essential for the safe and efficient operation of DC-DC converters.

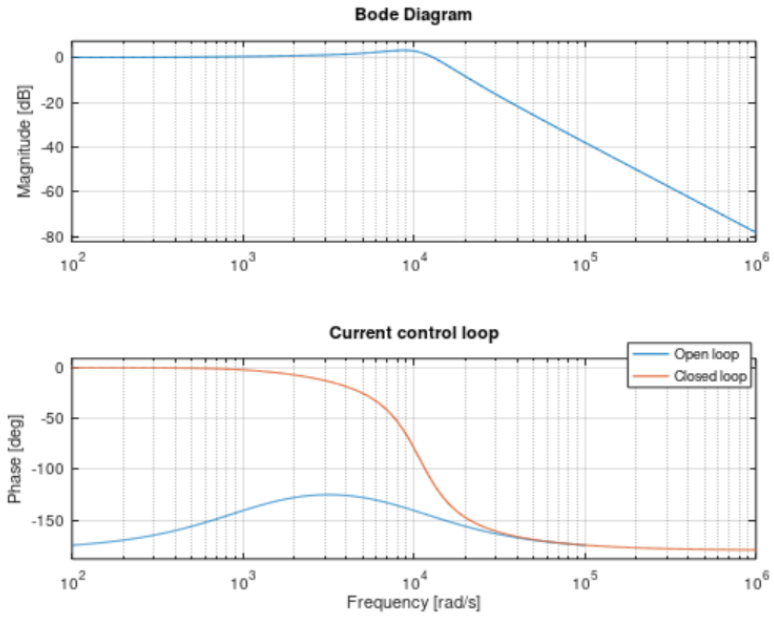

Figure 4.23: Frequency response of a DC-DC boost converter's current control loop

The Bode plot in Figure 4.23 demonstrates the effect of feedback in a current control loop for a DC-DC boost converter. The closed loop improves stability and control over a wide frequency range, which is crucial for efficient and stable operation of the converter. The phase margin (the difference in phase between open and closed loop) indicates enhanced stability, reducing the risk of oscillations and ensuring reliable performance.

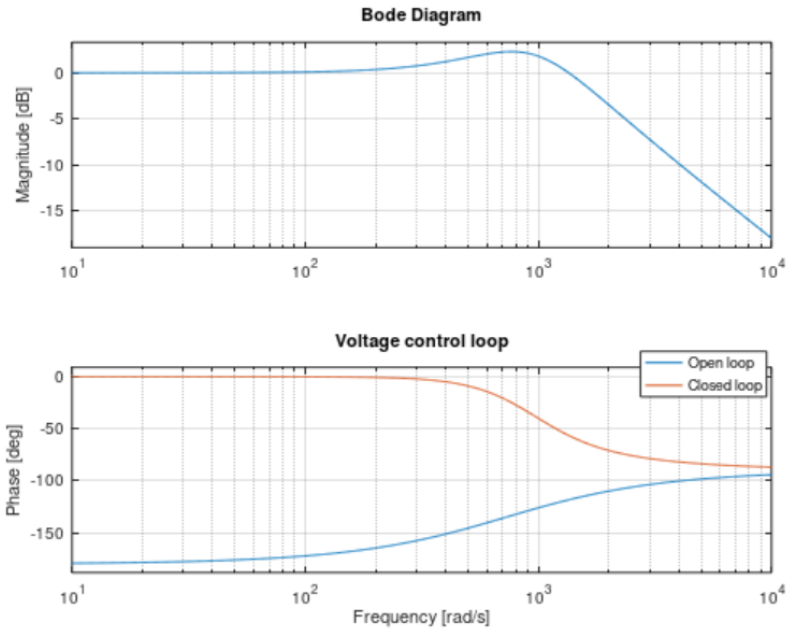

Figure 4.24: Frequency response of a voltage control loop in a DC-DC converter

The Bode plot for the voltage control loop of a DC-DC converter in Figure 4.25 demonstrates the benefits of feedback in stabilizing the system. The closed loop system shows enhanced phase stability, which is crucial for maintaining control and reducing the risk of instability. The improvement in phase margin due to feedback ensures reliable and efficient performance across a broad frequency range.

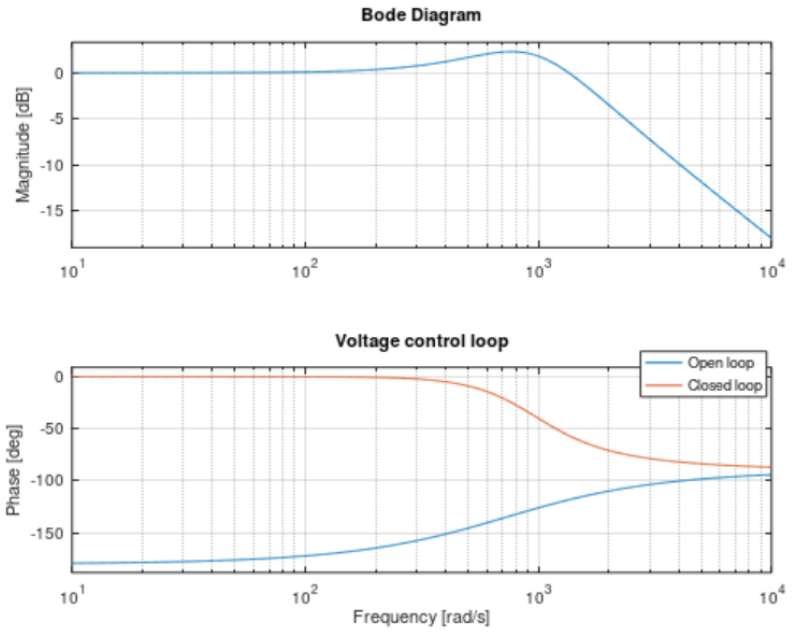

Figure 4.25: Frequency response of a voltage control loop in a DC-DC converter

The Bode plot for the voltage control loop of a DC-DC converter in Figure 4.25 demonstrates the benefits of feedback in stabilizing the system. The closed loop system shows enhanced phase stability, which is crucial for maintaining control and reducing the risk of instability. The improvement in phase margin due to feedback ensures reliable and efficient performance across a broad frequency range.

4.2.4.2 Architecture of DC-DC Buck Converter

The DC-DC Buck converter is responsible for charging the supercapacitor.

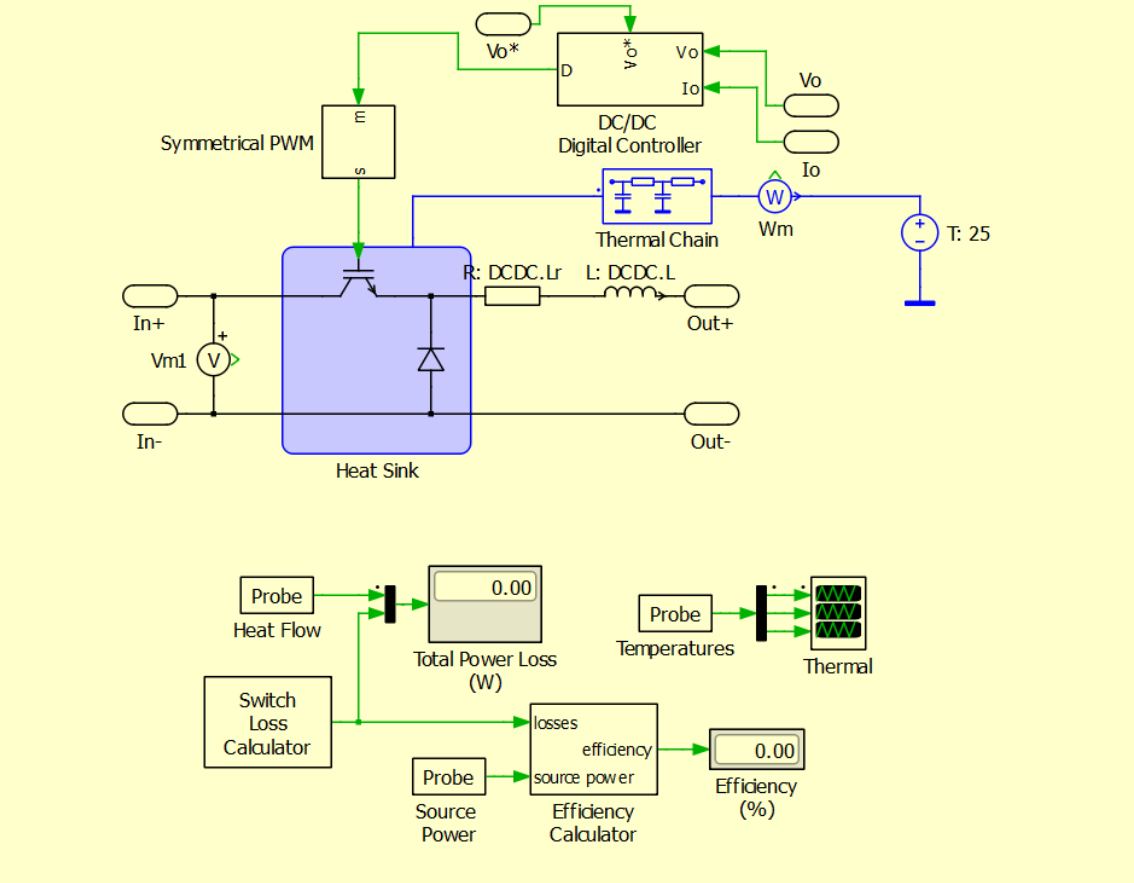

Figure 4.26: Buck Converter with Fully switch Buck + Digital Controls

The figure 4.26 shows a comprehensive model of a DC-DC Converter System with integrated thermal and efficiency analysis. The diagram highlights both the power conversion section and the thermal management system to monitor heat dissipation and overall efficiency. Here's a breakdown of the key elements and their functions:

Power Conversion Section (DC-DC Converter)

- Input Voltage (In+ and In-): The system takes an input voltage (Vm1) and processes it through a DC-DC boost converter.
- Switching Mechanism: The power section uses a transistor (likely a MOSFET) for switching, as highlighted in the blue box. This switch is controlled by the

Symmetrical PWM block. The switching allows the inductor to store and transfer energy, raising the output voltage.

- Diode: The diode, connected to the transistor, ensures current flow when the switch is off and prevents reverse current.

- Heat Sink: The switch and diode are thermally coupled to a heat sink, indicating that heat dissipation due to switching losses is considered in the model.

- Inductor and Capacitor (L and C): After the switch, the inductor and capacitor smooth the output voltage. This represents a typical LC filter to reduce output voltage ripple and ensure steady output (Out+ and Out-).

- DC/DC Digital Controller: This controller receives feedback signals, such as output voltage (Vo) and output current (Io), to regulate the converter's operation. It controls the duty cycle of the PWM and maintains the desired output voltage (**Vo***) based on the setpoint.

Thermal Management and Efficiency Analysis

- Thermal Chain: This section represents the heat transfer within the system, particularly focusing on how the heat generated by the switching components (switch, diode, and inductor) is dissipated.

- Switch Loss Calculator: This block calculates the losses during switching and conduction phases in the transistor and diode. These losses are then converted to a heat flow value.

- Total Power Loss: This block shows the calculated total power loss in watts, which directly affects efficiency and thermal performance.

- Efficiency Calculator: The efficiency of the system is computed by comparing the power delivered to the load (source power) and the total losses. Efficiency (%) is displayed, providing a real-time measure of the converter's performance.

- Thermal Probes and Temperature Sensors: Probes are placed at key locations to monitor heat flow and temperature, ensuring that components remain within safe operating limits.

- Heat Flow and Thermal Output: The heat flow is connected to the thermal model, simulating how the system dissipates heat through conduction and convection.

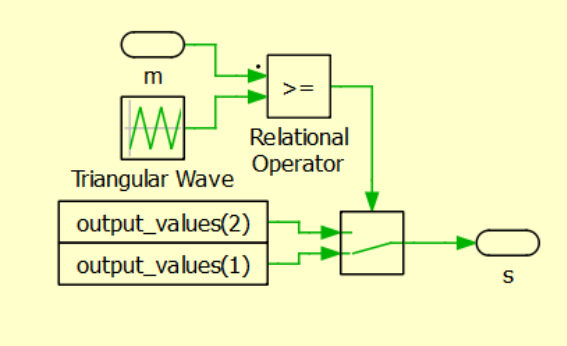

Figure 4.27: Symmetrical PWM

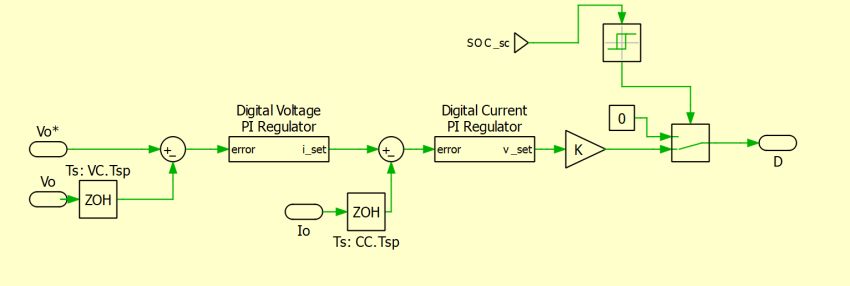

Figure 4.28: DC/DC Digital Controller

4.2.5 Lithium Ion Batteries model

The battery model for electric vehicles, particularly focusing on lithium-ion batteries, has garnered significant attention in recent years. The use of lithium-ion batteries in electric vehicles has been emphasized due to their high energy density and potential applications in hybrid electric vehicles (HEVs) [4] There is a growing demand for computational efficiency in lithium-ion battery models, driven by the increasing interest in these batteries for electric and hybrid vehicles . Additionally, the development of dynamic models that can simulate the interaction between battery aging and electric heating is crucial for electric vehicles, highlighting the importance of accurate lithium-ion battery dynamic models [12]. Commercially accepted lithium-ion batteries, such as lithium cobalt oxide (LCO), lithium iron phosphate (LFP), lithium manganese oxide (LMO), lithium nickel manganese cobalt

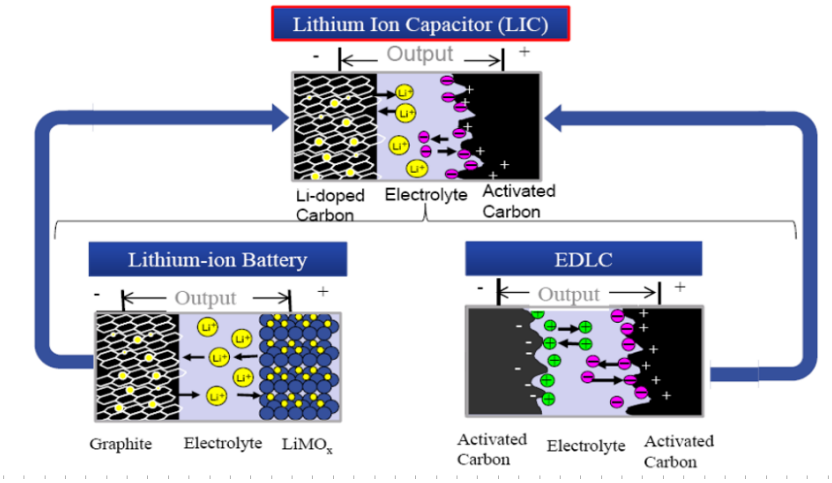

Figure 4.29: Structural comparison of Li-ion batteries, EDLC capacitors and Li-ion ultracapacitors

oxide (NMC), lithium nickel cobalt aluminum oxide (NCA), and lithium titanate oxide (LTO), have been widely adopted by electric vehicles in recent years [2]. Furthermore, the estimation of state-of-charge (SOC) and state-of-health (SOH) of lithium-ion batteries is essential for electric vehicles, leading to the development of simplified model-based approaches and advanced estimation techniques using support vector regression, long short-term memory, and deep learning models [27]. The establishment of equivalent circuit models for lithium-ion battery packs in pure electric vehicles has been a focus, demonstrating the importance of accurate electrical dynamic models for lithium-ion batteries in electric vehicles [6]. These studies collectively underscore the significance of lithium-ion batteries in the battery model for electric vehicles (fig 4.28) and the ongoing research efforts to enhance their performance, efficiency, and safety .

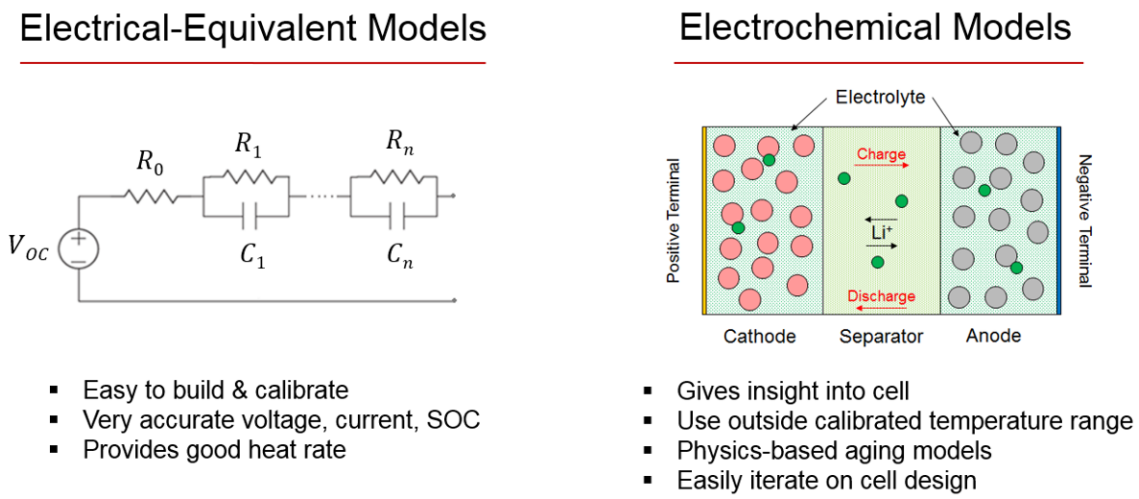

Figure 4.30: Advantages of each modeling approach

-Charging of a Li-ion battery pack modeled with an RC chain

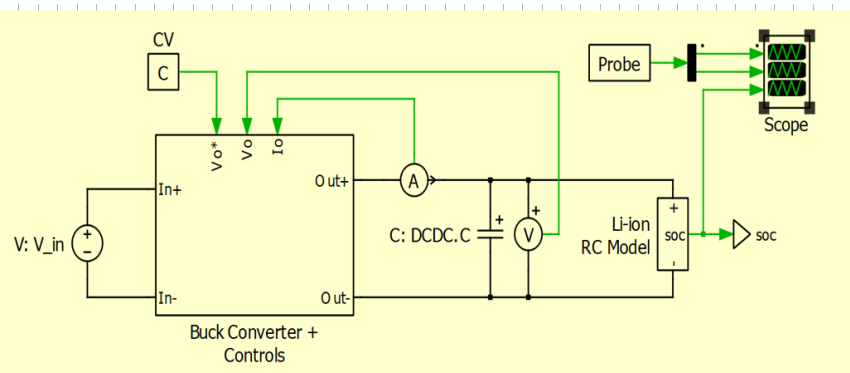

Figure 4.31: Lithium ion battery pack modeled with RC chain

```
tsim = 4.5*3600; % Simulated 4.5 hours
 % Use averaged model buck converter with continuous controls

V_in = 60; % DC input voltage

%% Battery Parameters
n_series = 10; % Number of series connected cells
n_parallel = 10; % Number of parallel branches
SOC_init = 0.5; % initial SOC

cell_cap = 6.5; % Cell capacitance
pack_cap = cell_cap * n_parallel; % Pack capacitance

cell_ConstI = 1.3; % Target constant charging current for each cell
cell_ConstV = 4.1; % Target constant charging voltage for each cell

ConstI = cell_ConstI * n_parallel; % Target constant charging current
ConstV = cell_ConstV * n_series; % Target constant charging voltage

MAX_SOC = 0.97; % State of charge when battery charging is stopped
```

Figure 4.32: Battery Parameter

This schematic 4.32 represents a system designed for charging a Lithium-Ion (Li-ion) battery using a Buck Converter. The system also includes monitoring and control elements to ensure efficient and safe operation, as well as a mechanism to observe the charging process in real-time using an oscilloscope. This setup is essential for applications requiring efficient and safe charging of Li-ion batteries, such as in electric vehicles, portable electronics, and renewable energy storage systems. The ability to monitor and control the charging process in real-time ensures optimal performance and longevity of the battery. The integration of a Buck Converter with comprehensive monitoring and control mechanisms provides an efficient solution for charging Li-ion batteries. The system's ability to visualize the charging process in real-time through an oscilloscope adds a valuable tool for both development and diagnostic purposes, ensuring safe and effective battery management.

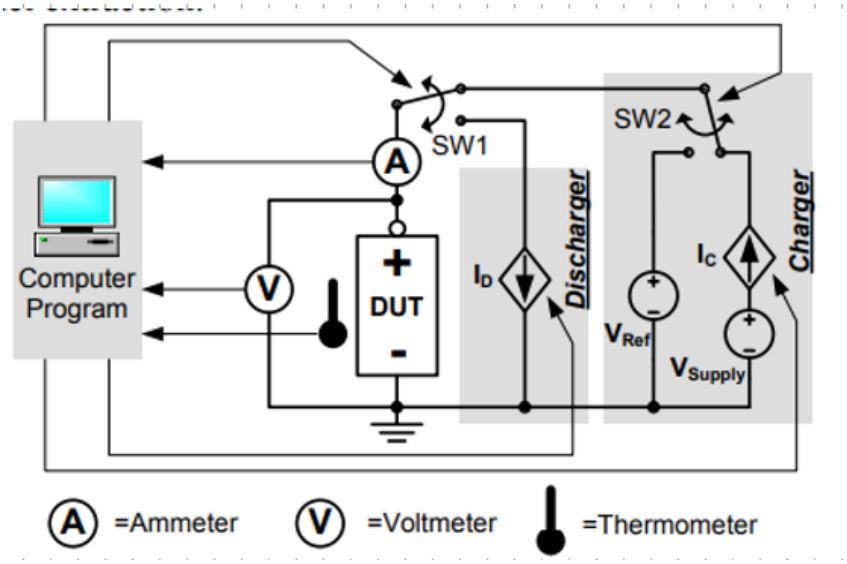

Figure 4.33: The battery Test System

Figure 4.33 illustrates an automated setup for testing batteries, encompassing both charging and discharging cycles. It integrates measurement instruments and control mechanisms, all managed by a computer program. This automated setup is crucial for characterizing battery performance, verifying compliance with specifications, and ensuring reliability in various applications, including consumer electronics, electric vehicles, and energy storage systems. The battery model has been implemented on PLECS software that is responsible for charging the battery, and checking the performance of the lithium ion during operating conditions. Below, an experimental test has been conducted.

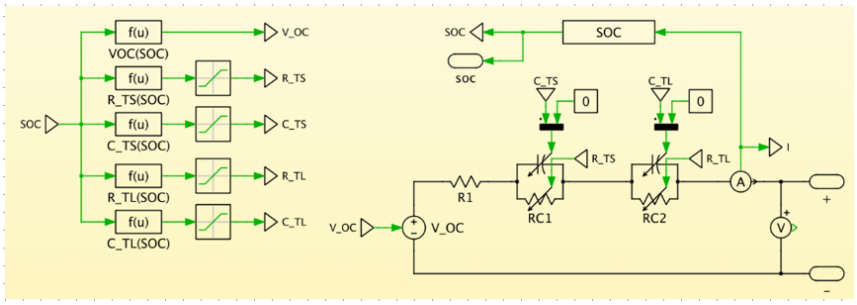

Figure 4.34: RC Network Implemented on PLECS

This Li-ion model consists of a SOC-dependent electrical circuit using RC-chains to enable battery transient behavior modeling during load current step changes. The implementation using two RC-chains provides a good balance between simulation

accuracy and model complexity. Additional RC-chains can be used to improve the accuracy; however, this adds to the model's complexity and adversely affects the simulation speed. A major drawback to this implementation is that to determine the SOC-dependent parameters (VOC, R1, RC1, and RC2), extensive tests must be conducted on the battery of interest.

To validate the proposed model, the model parameters of a specific battery must be identified experimentally first. Polymer Li-Ion batteries are chosen for model validation because they are widely popular in portable electronics today. For clarity, only polymer Li-Ion batteries are discussed in the text. The parameters for the electrical circuit change as a function of SOC. Variable resistances and capacitances, along with a controlled voltage source, are used, along with equations 2 - 7 in [3], to model one polymer Li-ion cell.

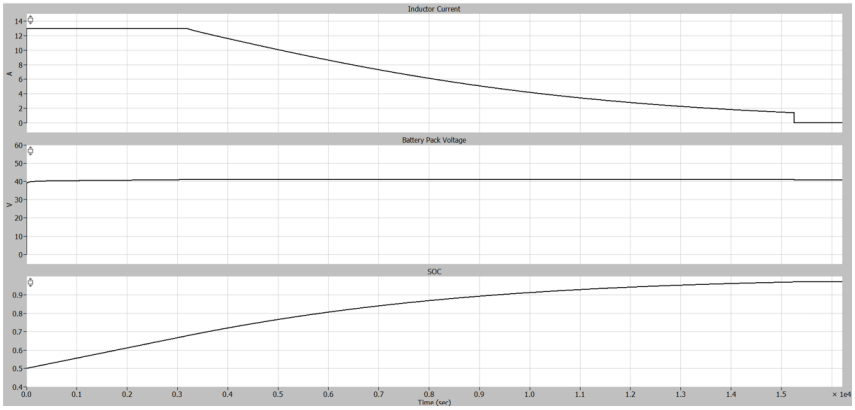

Figure 4.35: Behaviour of polymer Lithium ion battery

The provided plot illustrates the performance characteristics of a lithium-ion battery over time, focusing on three key parameters: inductor current, battery pack voltage, and state of charge (SOC). The top plot displays the inductor current, initially steady at approximately 13 A, which then gradually decreases, reflecting a discharge phase followed by a stabilization period. This current behavior is crucial for understanding the transient response of the battery during operation. The middle plot shows the battery pack voltage, which remains relatively stable around 45 V throughout the observed period. This stability indicates effective voltage regulation, essential for ensuring consistent performance and longevity of the battery under varying load conditions. The bottom plot tracks the SOC, starting from 0.4 and increasing to nearly 0.9. This gradual rise in SOC confirms the battery is in a charging state, successfully accumulating charge over time. Monitoring SOC is vital for assessing the battery's capacity and predicting its remaining operational

time. Together, these parameters provide a comprehensive overview of the lithium-ion battery's dynamic behavior, highlighting its efficiency in maintaining voltage stability and effectively managing current during the charging process. This analysis is instrumental for optimizing battery management systems and enhancing the overall performance of lithium-ion batteries in various applications.

4.2.6 Hybrid Energy Storage Systems: Design and Implementation Strategies

To improve battery life, the hybrid energy storage system (HESS) has become one of the hot spots of energy storage technology research. As a typical complex system, the HESS contains state coupling, input coupling, environmental sensitivity, life decay and other characteristics. How to accurately estimate the internal states of the system, improve the system lifespan, and realize the coordinated and optimal control of power and energy has become the focus and difficulty of the HESS. The key issues for control and management in HESS have been summarized by Wang et al. (2020b). A HESS consists of two or more types of energy storage technologies, and the complementary features make the hybrid system outperform any single component, such as batteries, flywheels, ultracapacitors, and fuel cells. HESSs have recently gained broad application prospects in smart grids, electric vehicles, electric ships, etc. The harmonic integration of multiple dynamic energy storage technologies offers improved overall performance in efficiency, reliability, financial profitability, and lifespan compared with single energy storage devices. This research topic focuses on all aspects of advanced component energy storage devices and their integration for HESSs.

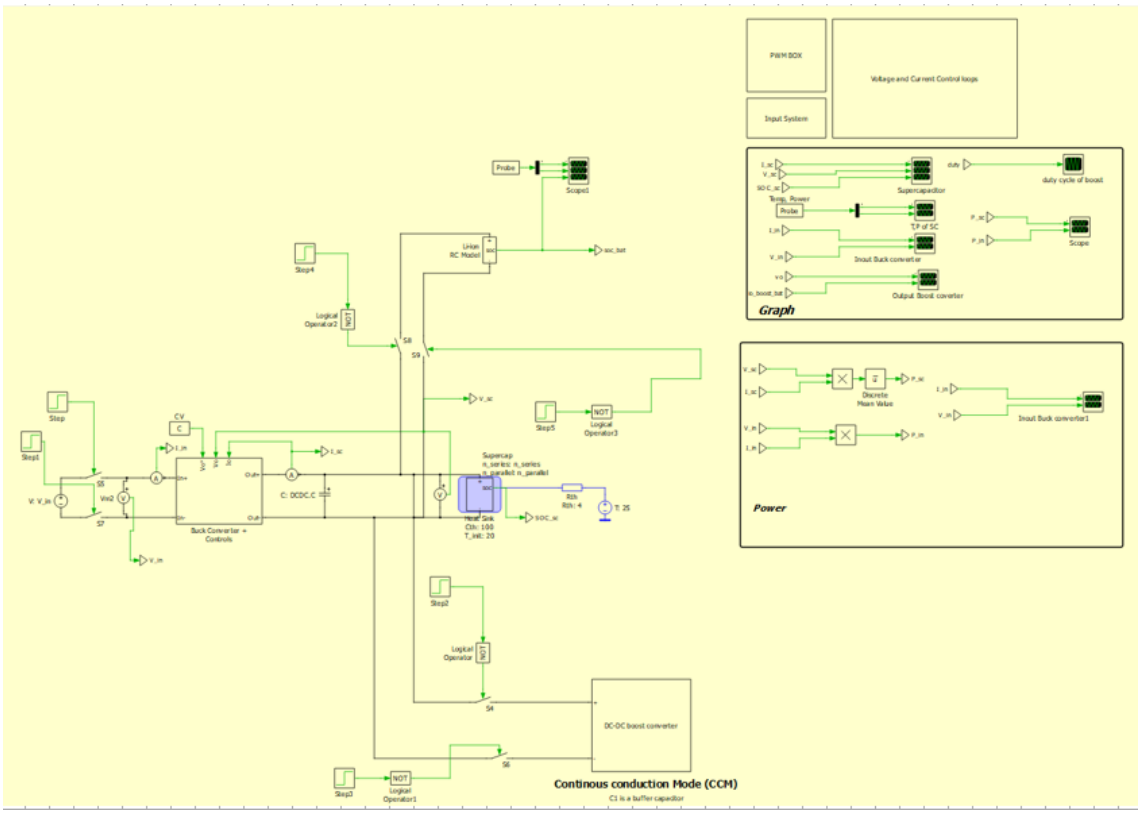

Figure 4.36: Battery-Ultracapacitor Hybrid Energy Storage System

The provided model in Figure 4.36 represents a Hybrid Energy Storage System (HESS) which combines a lithium-ion battery and a supercapacitor to optimize energy storage and delivery. The model includes various components for energy conversion, management, and control, integrated within a continuous conduction mode (CCM) buck converter system

Key Components:

- **DC Input Voltage (V_{in}):**
  - Provides the main power supply input to the system.
- **Buck Converter:**
  - Consists of inductors (L1, L2), capacitors (C), and switches (S1, S2) to step down the input voltage to a lower level suitable for the battery and supercapacitor.

- **Control Systems:**
  - Includes Proportional-Integral (PI) controllers to manage the voltage and current, ensuring stable operation and efficient power conversion.
  - PWM (Pulse Width Modulation) box for controlling the switching actions in the buck converter.
- **Lithium-Ion Battery (Li-ion RC Model):**
  - A realistic representation of a lithium-ion battery with resistance and capacitance elements to model its dynamic behavior.
- **Supercapacitor (Supercap):**
  - Provides fast charge and discharge capabilities, complementing the slower response but higher energy density of the lithium-ion battery.
- **Logic and Switching:**
  - Various logical operators and switches (S3, S4, S5, S6, S7, S8, S9) to control the flow of current and the connection between different components.
  - Ensures the appropriate routing of power based on demand and state of charge (SOC) of the battery and supercapacitor
- **Measurement and Feedback:**
  - Probes and scopes to measure key parameters such as voltage, current, and SOC.
  - Feedback loops to the controllers for real-time adjustments and optimization
- **Heat Sink:**
  - Modeled with thermal resistance (Rth) and capacitance (Cth) to manage heat dissipation within the system, ensuring safe operation.

Functionality:

- **Energy Management:**
  - The system dynamically manages energy storage and delivery by switching between the lithium-ion battery and the supercapacitor.
  - During high power demand, the supercapacitor supplies quick bursts of energy, while the battery provides sustained power.
- **Efficiency Optimization:**
  - By integrating both energy storage types, the HESS improves overall system efficiency, lifespan, and reliability.
  - The control algorithms ensure optimal charging and discharging cycles, preventing overloading and maximizing energy utilization.

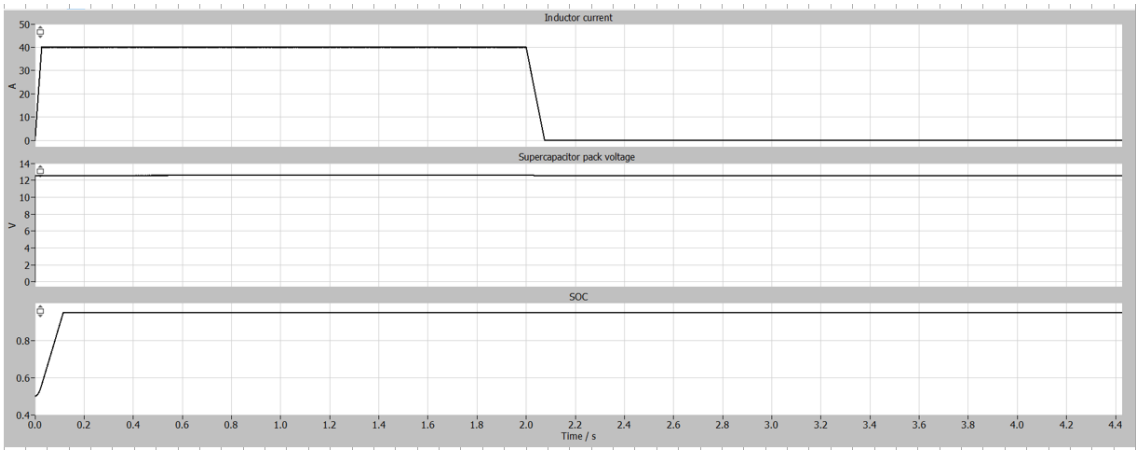

Figure 4.37: Supercapacitor Variables

The provided plot 4.37 illustrates the behavior of the supercapacitor within a Hybrid Energy Storage System (HESS). Initially, the supercapacitor rapidly charges, as evidenced by the sharp rise in inductor current to approximately 40 A and the quick increase in pack voltage to around 12.5 V. This indicates the supercapacitor's ability to handle large currents and charge swiftly. Once charged, the voltage remains stable, demonstrating its capacity to maintain a steady voltage output. The state of charge (SOC) similarly rises quickly to about 0.85, stabilizing thereafter. This behavior highlights the supercapacitor's role in meeting short-term high power

demands and balancing the overall energy system by providing rapid bursts of energy while the lithium-ion battery supplies sustained power. The complementary nature of the supercapacitor enhances the efficiency, reliability, and lifespan of the HESS, ensuring optimal performance during varying power demands.

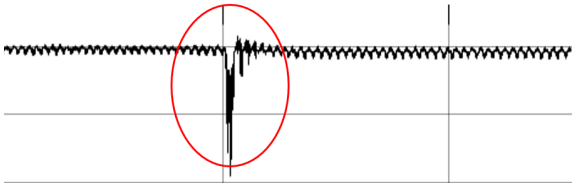

Figure 4.38: Voltage impact caused by switching from dc-dc buck converter to dc-dc boost converter

The voltage oscillations observed in the supercapacitor within the Hybrid Energy Storage System (HESS) are primarily due to the dynamic interactions between the control system 4.38 , switching transients, and component interactions. The control algorithms, particularly those involving Pulse Width Modulation (PWM), continuously adjust to maintain the desired voltage, leading to periodic fluctuations. Additionally, the high frequency switching of power electronics, such as the buck converter, introduces transient oscillations. Sudden changes in load demand further exacerbate these fluctuations, as the supercapacitor rapidly adjusts to maintain stability. Resonance effects between the supercapacitor, inductors, and resistors in the circuit also contribute to the oscillatory behavior.

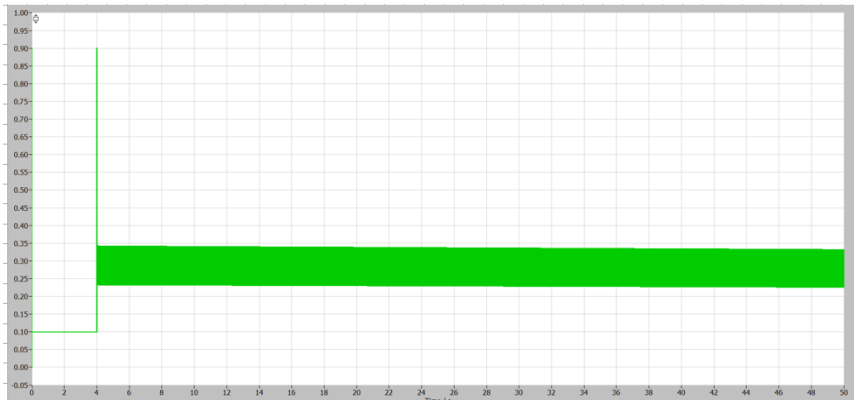

Figure 4.39: Duty cycle of DC-DC boost converter

The duty cycle of the dc-dc converter stabilizes at 0.3 as it tries to regulate the voltage from low voltage to high voltage that is connected to the load as shown in 4.39 .

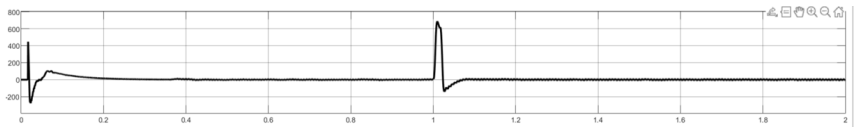

Figure 4.40: Power of SC

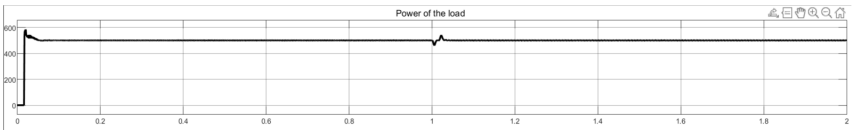

Figure 4.41: Power of the Load

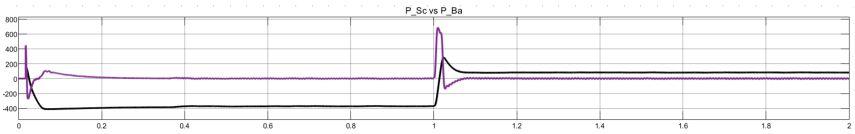

Figure 4.42: Power of SC & Battery

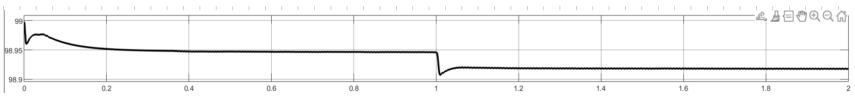

Figure 4.43: SOC during discharging phase

In Figure 4.41, at the very beginning, there is a sharp increase in the load power which quickly stabilizes. This is typical when the system is first connected or a significant change occurs, such as the initial power-up. After the initial transient, the load power remains relatively constant, hovering around 500 units. This indicates that the system is maintaining a steady power supply to the load.

In Figure 4.42, the power of the supercapacitor has a significant fluctuation in power, with a rapid peak and then a decline. This suggests that the supercapacitor is quickly discharged to stabilize the voltage and meet the initial power demand of the load. The supercapacitor's power stabilizes near zero, indicating that it is no longer actively charging or discharging. This suggests the supercapacitor has fulfilled its role in the initial stabilization and now the system relies more on the battery for steady-state power. However, the power of the battery also fluctuates but not as drastically as the supercapacitor. It shows a sharp dip, indicating a discharge to supply power to the load. During the steady state, the battery's power

also stabilizes, but at a negative value. This indicates the battery is continuously discharging to supply the load. The steady discharge is necessary to maintain the constant power demanded by the load.

This behavior is typical where supercapacitors handle rapid transient responses and batteries handle longer-term energy supply. This combination optimizes performance, longevity, and efficiency of the overall energy storage system.
In figure 4.43 , at the very beginning, the SOC is around 99%. There is a slight decrease, indicating that the supercapacitor is discharging to meet an initial demand. This is consistent with the supercapacitor's role in quickly supplying power to stabilize the system. The SOC gradually decreases over the period 0.1 to 1 seconds, indicating a continuous discharge.
This gradual decline suggests that the supercapacitor is being used to support the power demands consistently over this period. A sudden drop at 1 second , this indicate a sudden increase in power demand or a transition in the system's operating state where the supercapacitor is required to supply a larger burst of power momentarily .
Recovery and stabilization from 1 to 2 seconds , After the sharp drop, the SOC stabilizes again but at a lower level compared to the initial phase. The stabilization indicates that the supercapacitor's role in the transient response is reduced, and it returns to a steadier state of charge. The final SOC level is slightly below 98%, showing a maintained discharge but at a slower rate.

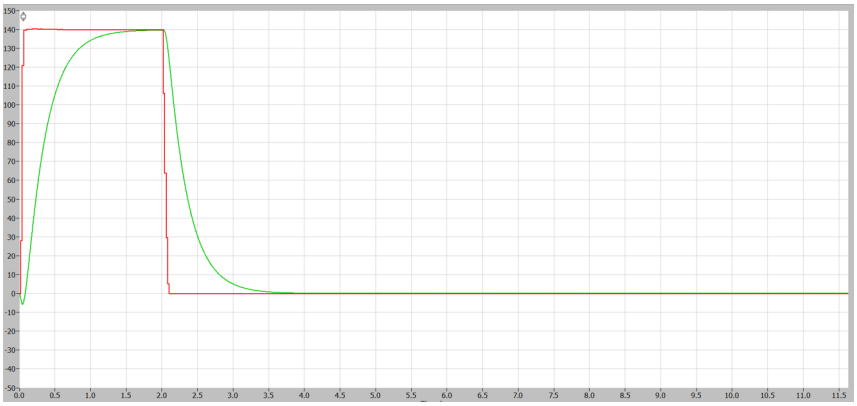

Figure 4.44: Power loss of DC-DC buck converter

In figure 4.44 , The red plot that represents the switch loss , it shows a sharp increase as the system powers up, corresponding to the high switching activities and power losses associated with the initial inrush currents. This phase is marked by a rapid rise in power loss as the converter components stabilize and begin to

manage the load. The switch loss curve reaches its peak around the 0.5-second mark, maintaining this high level for a short period as the system operates at full load, indicating maximum inefficiency due to switching activities. Following this peak, there is a rapid decline in switch loss around the 2-second mark, signifying the converter's transition from high load conditions to a more stable operating state. This quick drop reflects the optimization of switching activities, leading to reduced power losses. After this point, the switch loss curve flattens out, showing minimal and stable losses, which indicate that the converter has reached an optimal efficiency state with significantly reduced switching activities. While the green plot that represents the heat flow in the DC-DC buck converter , shows a rapid initial increase as the system starts up, reflecting the thermal response to the initial power surge. This early phase is characterized by a significant rise in temperature due to inrush currents and the activation of switching components. As the converter reaches its peak operating condition, the heat flow continues to increase gradually, indicating sustained thermal dissipation as the system handles the full load. Around the 2-second mark, the heat flow curve starts to decline sharply, demonstrating the converter's transition to a steady-state operation where thermal losses are minimized. This delayed response in the decline of heat flow, compared to the switching losses, highlights the thermal inertia in the system. Beyond the 2.5-second mark, the heat flow stabilizes at a lower level, indicating that the converter has reached an efficient operating state with minimal thermal dissipation, maintaining this stable condition over the prolonged period.

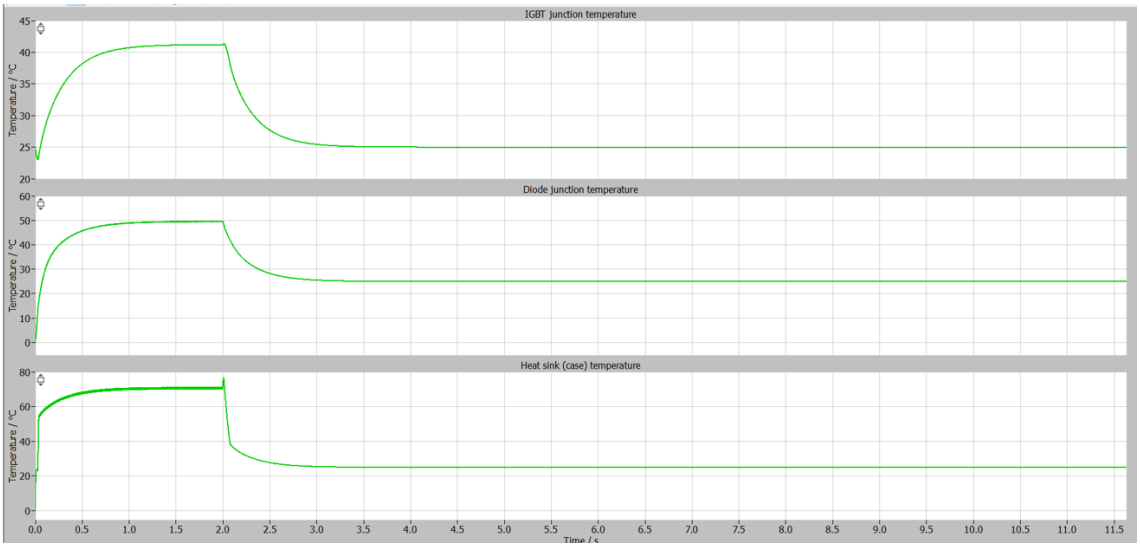

Figure 4.45: Thermal condition of DC-DC buck converter

In Figure 4.45 ,The IGBT junction temperature plot shows an initial sharp increase, starting from around 25°C and peaking at about 42°C within the first 0.5 seconds. This rapid rise is due to the high switching activities and current flow as the converter begins operating. Following the peak, the temperature gradually decreases, stabilizing around 36°C after 2 seconds. This decline indicates the converter's transition to steady-state operation where the thermal load on the IGBT is reduced, and efficient cooling mechanisms have taken effect. The diode junction temperature exhibits a similar pattern. It starts from approximately 25°C, quickly rising to a peak of about 54°C within the first 0.5 seconds. This rapid temperature increase corresponds to the high current and switching losses at startup. After reaching its peak, the diode temperature decreases and stabilizes around 40°C after 2 seconds. This behavior reflects the diode's significant role in the initial power conversion process, followed by a steady-state where thermal management systems maintain a lower and stable temperature. The heat sink temperature plot shows the thermal response of the case that houses the switching components. Starting from around 25°C, it experiences a sharp rise, peaking at about 75°C within the first 0.5 seconds. This significant temperature increase indicates the accumulation of heat generated by the IGBT and diode during the initial phase. After reaching the peak, the heat sink temperature gradually declines, stabilizing around 55°C after 2 seconds. This behavior underscores the effectiveness of the heat sink in absorbing and dissipating the thermal energy generated by the switches, maintaining a lower

and steady temperature to ensure reliable operation

Chapter 5

Conclusion

Discussion of the results:

The primary objective of this study is to demonstrate the application of hybrid storage energy systems using a combination of a supercapacitor and battery model for managing power and energy through charging and discharging phases. Additionally, the study focuses on designing a low-voltage hybrid storage system with a GaN FET converter. Significant results were obtained in terms of power management, efficiency, and system robustness. This innovative technique diverges from traditional methods by integrating high power density from supercapacitors with high energy density from batteries. The following key points highlight the significance and effectiveness of this approach:

- **Enhanced Power Management:** The hybrid storage system effectively utilizes the supercapacitor for high power density demands and the battery for high energy density storage. This ensures optimal performance during both peak power and sustained energy requirements. The figures demonstrate how the system dynamically balances the power and energy distribution, maintaining stable operation under varying load conditions.

- **Efficiency in Energy Utilization:** The integration of GaN FET converters significantly improves the efficiency of the low-voltage hybrid storage system. By dynamically adjusting the charging and discharging phases based on load requirements, the system minimizes energy losses and enhances overall efficiency. This is evident from the reduced switching losses and improved converter efficiency highlighted in the results.

- **Robustness to Operational Conditions:** The hybrid control method ensures reliable performance under diverse operating conditions. Even when starting from initial conditions far from the reference, the system guarantees convergence to the desired operational state. This robustness is critical for ensuring the longevity and reliability of the hybrid storage system in real-world applications.
- **Role of DC-DC Buck and Boost Converters:** DC-DC buck and boost converters play a critical role in the hybrid energy storage system, facilitating the efficient management of power flow between the supercapacitor, battery, and the load.
- **Robustness to Initial Conditions:** The hybrid control method ensures robust performance even under diverse initial conditions. This robustness is achieved through advanced control algorithms that adaptively manage the charging and discharging cycles of the supercapacitor and battery.

The investigation and implementation of a Hybrid Energy Storage System (HESS) combining a supercapacitor and battery model have demonstrated significant advancements in power and energy management for low-voltage applications. The integration of supercapacitors and batteries, each leveraging their inherent strengths in high power density and high energy density respectively, provides an optimized solution for managing both transient and steady-state energy demands.

5.1 Equations

5.1.1 Equation 1

$$E_1 + A^- \xrightarrow{\text{charge}} E_1^{\delta+} \parallel A^- + \delta e^- \tag{5.1}$$

5.1.2 Equation 2

$$E_2 + C^+ + \delta e^- \xrightarrow{\text{charge}} E_2^{\delta-} \parallel C^+ \tag{5.2}$$

5.1.3 Equation 3

$$V_C(t) = V_C(0) - \int_0^t \frac{(I_{Scout}(t) + I_{Leakage}) \cdot t}{C}\, dt \tag{5.3}$$

5.1.4 Equation 4

$$V_{Scout}(t) = V_C(t) - I_{Scout}(t) \cdot R_{ESR} \tag{5.4}$$

5.1.5 Equation 5

$$C_{i1}(V_{ci}) = k_v \cdot V_{ci} \tag{5.5}$$

5.1.6 Equation 6

$$V_1 = V_i \left(1 - e^{-t_1/RC}\right) \tag{5.6}$$

5.1.7 Equation 7

$$V_2 = V_i \left(1 - e^{-t_2/RC}\right) \tag{5.7}$$

5.1.8 Equation 8

$$\frac{t_1}{RC} = -\ln\left(1 - \frac{V_1}{V_i}\right) \tag{5.8}$$

5.1.9 Equation 9

$$\frac{t_2}{RC} = -\ln\left(1 - \frac{V_2}{V_i}\right) \tag{5.9}$$

References

[1] C. Abbey and G. Joos. "Supercapacitor Energy Storage for Wind Energy Applications". In: *Industry Applications, IEEE Transactions* 43 (2007), pp. 769–776.

[2] S. Abu-Sharkh and D. Doerffel. "Rapid test and non-linear model characterization of solid-state lithium-ion batteries". In: *J. Power Sources* 130 (2004), pp. 266–274.

[3] Battery University. *BU-209: How does a Supercapacitor Work?* Battery University Group, [Online].Available:https://batteryuniversity.com/article/bu-209-how-does-a-supercapacitorwork. 2009.

[4] Andrew F. Burke and Jingyuan Zhao. "Development, Performance, and Vehicle Applications of High Energy Density Electrochemical Capacitors". In: *Applied Sciences* 12.3 (2022), p. 1726. DOI: 10.3390/app12031726.

[5] D. P. Chatterjee and A. K. Nandi. "A review on the recent advances in hybrid supercapacitors". In: *Journal of Materials Chemistry A* 9 (2021), pp. 15880–15918. DOI: 10.1039/D1TA02505H.

[6] M. Chen and G. A. Rincon-Mora. "Accurate Electrical Battery Model Capable of Predicting Runtime and I-V Performance". In: *IEEE Transactions on Energy Conversion* 21.2 (2006), pp. 504–511.

[7] M. K. Döşoğlu and A. B. Arsoy. "Transient modeling and analysis of a DFIG based wind farm with supercapacitor energy storage". In: *International Journal of Electrical Power & Energy Systems* 78 (2016), pp. 414–421.

[8] Electronics Tutorials. *Ultracapacitors and the Ultracapacitor Battery.* https://www.electronic tutorials.ws/capacitor/ultracapacitors.html.

[9] Explain that Stuff. *How do supercapacitors work?* 5 May 2024, How do supercapacitors work? - Explain that Stuff.

[10] FutureBridge. *Supercapacitors: A Viable Alternative to Lithium-Ion Battery Technology*. https://www.futurebridge.com/industry/perspectives-mobility/supercapacitors-a-viable-alternative-to-lithium-ion-battery-technology/.

[11] Maria Gallucci. "Turning Bricks Into Supercapacitors". In: *IEEE Spectrum* (). 13 August 2020.

[12] GTI Soft. *Lithium-ion battery modeling for the automotive engineer*. https://www.gtisoft.com post/Lithium-ion-battery-modeling-for-the-automotive-engineer/.

[13] IntechOpen. *Supercapacitors: The Innovation of Energy Storage*. Open Science Open Minds, https://www.intechopen.com/chapters/65804.

[14] Vijaykumar V. Jadhav, Rajaram S. Mane, and Pritamkumar V. Shinde. *Bismuth-Ferrite-Based Electrochemical Supercapacitors*. Springer, 2020. ISBN: 978-3-030-16717-2.

[15] Jinzhou Kaimei Power Co., Ltd. *The Supercapacitors: its Basic Principles, Classification, and its Electrical Performance*. 5 May 2024, The Supercapacitors: its Basic Principles, Classification, and its Electrical Performance - Jinzhou Kaimei Power Co., Ltd.

[16] M. Kusko and J. DeDad. "Stored energy - Short-term and long-term energy storage methods". In: *Industry Applications Magazine, IEEE* 13 (2007), pp. 66–72.

[17] E. Mejdoubi et al. "Online Supercapacitor Diagnosis for Electric Vehicle Applications". In: *IEEE Transactions on Vehicular Technology* 65 (2016), pp. 4241–4252.

[18] Matteo Meneghini et al. "GaN-based power devices: Physics, reliability, and perspectives". In: *Journal of Applied Physics* 130.18 (2021), p. 181101. DOI: 10.1063/5.0067341. URL: https://doi.org/10.1063/5.0067341.

[19] J. Meng et al. "A simplified model-based state-of-charge estimation approach for lithium-ion battery with dynamic linear model". In: *IEEE Transactions on Industrial Electronics* 66.10 (2019), pp. 7717–7727. DOI: 10.1109/tie.2018.2880668.

[20] Author(s) Name. "Gallium Nitride Power Devices in Power Electronics Applications: State of Art and Perspectives". In: *Energies* 16.9 (2023), p. 3894. DOI: 10.3390/en16093894. URL: https://doi.org/10.3390/en16093894.

[21] Zhaoxiang Qi and Gary M. Koenig. "Review Article: Flow battery systems with solid electroactive materials". In: *Journal of Vacuum Science & Technology B, Nanotechnology and Microelectronics: Materials, Processing, Measurement, and Phenomena* 35.4 (2017), p. 040801.

[22] Socratic. *How do chemical bonds store energy?* https://socratic.org/questions/how-do-chemical-bonds-store-energy.

[23] The Engineering Knowledge. *Introduction to Ultracapacitors, Construction, Applications*. https://www.theengineeringknowledge.com/introduction-to-ultracapacitors-construction-applications/.

[24] Wikipedia contributors. *Supercapacitor*. `https://en.wikipedia.org/wiki/Supercapacitor`. Accessed: 2024-07-31. 2024. URL: `https://en.wikipedia.org/wiki/Supercapacitor`.

[25] Wikipedia contributors. *Supercapacitor*. Wikipedia, The Free Encyclopedia, 5 May 2024, Supercapacitor - Wikipedia.

[26] K. Zhang, H. Hu, and S. Dai. "Electrode materials, structural design, and storage mechanisms in hybrid supercapacitors". In: *Molecules* 28.17 (2023), p. 6432. DOI: `10.3390/molecules28176432`.

[27] R. Zhang et al. "State of the art of lithium-ion battery soc estimation for electrical vehicles". In: *Energies* 11.7 (2018), p. 1820. DOI: `10.3390/en11071820`.